UNITED ARAB REPUBLIC
ATOMIC ENERGY ESTABLISHMENT
REACTORS DEPARTMENT

THE COOLING OF A SIMULATED FUEL ELEMENT BY A FLOW OF NATURALLY CIRCULATED BOILING WATER

By

N. RAAFAT, M. EL FOULY
E. S. GADLIS and M. KHATTAB

1971

UNITED ARAB REPUBLIC

ATOMIC ENERGY ESTABLISHMENT

REACTORS DEPARTMENT

————————

THE COOLING OF A SIMULATED FUEL ELEMENT BY A

FLOW OF NATURALLY CIRCULATED BOILING WATER

By

N. RAAFAT, M. EL-FOULY,

E.S. GADDIS and M. KHATTAB

1971

C O N T E N T S

A B S T R A C T

Experimental investigation of the cooling of a uniformly heated tube, forming the heating surface of an annular space and presenting a simulated fuel element, by naturally circulated boiling water was presented in this report.

It was shown that accurate prediction of the surface temperature of the heater cannot be made without taking into consideration entrance and end effects. This can be especially important in case of short heaters, where the entrance length may be a considerable part of the total heater length. The wall surface temperature in the subcooled region can be predicted by a knowledge of the heat transfer coefficient in the convection and nucleate boiling regions.

The rate of increase of coolant mass flow rate with increase in inlet coolant temperature (also with increase in power) increased considerably once net boiling started in the test section. However, this rate of increase decreased to low level, once the steam quality at the exit exceeded certain value. At atmospheric conditions, the corresponding exit steam quality can be as low as 0.03, and is attributed to the high void fraction and low rate of its increase at such low steam quality. Such behaviour can be important in predicting the performance of natural circulation boiling reactors.

The effect of diameter ratio on the temperature distribution of the heater was insignificant, and was mainly in the entrance region.

The coolant mass flow rate showed a maximum at the intermediate diameter ratio.

N O T A T I O N

A heater surface area.

c specific heat of water.

D_i inside diameter of annulus, or outer diameter of heater tube.

D_o outside diameter of annulus, or internal diameter of glass jacket.

D_e equivalent diameter.

h heat transfer coefficient.

h_c heat transfer coefficient in the convection region.

h_s heat transfer coefficient in the subcooled region.

h_n heat transfer coefficient in nucleate region.

$h_{\ell f}$ heat transfer coefficient in the two phase flow region (region 4).

$h_{\ell fm}$ maximum heat transfer coefficient at the end of region 4.

K liquid thermal conductivity.

L latent heat of evaporation.

ℓ total heater length.

ℓ_b boiling length.

ℓ_c convection length.

$\ell_{\ell f}$ length of the two phase flow region (region 4).

ℓ_{nb} non-boiling length.

ℓ_s subcooled boiling length.

N_u nusselt number.

P_r prandtl number.

Q heat input to test section.

q wall heat flux.

R_e reynolds number.

S slip ratio.

s heat transfer perimeter.

T temperature.

T_b coolant bulk temperature.

T_i inlet temperature to test section.

T_{sat} saturation temperature at the coolant pressure.

T_w wall surface temperature.

T_{wn} minimum wall surface temperature in the subcooled region.

V coolant velocity in test section.

W Coolant mass flow rate.

X steam quality.

X_e steam quality at the exit.

Z_c distance measured in the longitudinal direction of the heater from the beginning of the convection region.

Z_s same as Z_c, but from the beginning of the subcooled region.

Z_{sm} longitudinal distance in the subcooled region, where wall surface temperature is minimum.

Z_n same as Z_c, but from the beginning of the nucleate region.

$Z_{\ell f}$ same as Z_c, but from the beginning of region 4.

α steam void fraction.

α_e exit steam void fraction.

ρ_ℓ liquid density.

ρ_{md} average density in downcomer.

ρ_{mt} average density in test section.

ρ_v vapour density.

u_ℓ liquid dynamic viscosity.

ΔT_f film temperature drop.

1. INTRODUCTION

It was acknowledged, long ago, that boiling water reactors, as a heat source for power generation, have some important advantages over other types as the pressurized water and gas cooled reactors. This is partly due to possible elimination of some of the expensive items as the heat exchangers in the boiling system, and partly due to possible lower coolant pressure compared with the pressurized water type and lower pumping power requirements and pump capital cost compared with the gas cooled reactors. However, the developing of boiling water reactors has been initially retarded by the doubts present at that time, that using a boiling liquid as a reactor coolant might not lead to a safe, stable and reliable system, and the first power reactors, the world has seen, were either of the gas cooled or the pressurized water type. But from that time, when these early reactors started operation, extensive research work began to investigate the possibility of allowing boiling to occur inside the reactor core without affecting the high reliability and safe operation that should be built in them.

The most important thermal and hydraulic problems present in a boiling system, that reflect themselves on other aspects of the design of boiling water reactors are :

(1) Temperature attained at heating surfaces of fuel elements;
(2) Critical heat flux and its dependance on flow parameters;
(3) Density distribution in reactor core;
(4) Pressure drop in reactor channels;
(5) Hydraulic stability of the boiling system;
(6) Vapour-liquid separation.

While most of these problems are similar to those met in the design of conventional boilers, neverthless the degree of their importance may be greater in the case of nuclear boiling reactors.

Recently, the Reactors Department in the U.A.R. Atomic Energy Establishment began to have interest in boiling heat transfer and its application in reactor cooling. A research programme was made to cover some particular research points of general interest in this field. One of the problems included in this programme is to study the heat transfer from a reactor fuel element to a boiling liquid, and for this investigation a rig with a simulated reactor fuel element was designed and erected. This work represents an experimental investigation using the above mentioned rig. The investigation involve the cooling of the simulated fuel element by a natural flow of water obtained by virtue of the difference in densities between the fluid in the vertical test section (simulated fuel element) and a relatively cooler downcomer in the rig.

2. DESCRIPTION OF THE APPARATUS

A brief description of the rig is given hereafter, its full details are presented in $\boxed{1}$.

The rig was a closed loop, made from stainless steel, and consisted essentially of a test section, a condenser, preliminary heaters, a flow meter, a surge tank and a centrifugal pump. The pump was inserted in the loop for forced convection experiments, and hence was not used in the experiments presented in this report.

The test section consisted essentially of a glass jacket and a stainless steel tube, 90.5 cms long, used as a heater. The outside diameter of the heater was 1 cm and was kept constant at all runs. The inside diameter of the glass jacket was changed in three steps leading to diameter ratio of the annular space of the test section of 2, 2.5 and 3, a series of runs were made at each ratio. The working pressure of the rig was kept near atmospheric conditions by keeping the surge tank open to the atmosphere. The water entering the test section was slightly subcooled. The amount of subcooling was varied from 3 to 12°C.

Few runs were made with high subcooling leading to single phase flow in the test section. The fluid pressure was measured at inlet to and outlet of the test section by means of mercury manometers. Power regulation was made by voltage regulation across the heater tube. The power was 6.1 KW and the corresponding heat flux at the heater surface was 20.9 watt/cm^2. The surface temperature of the heater was measured by means of nine copper-constantan thermocouples embeded in the thickness of the heater at equal longitudinal intervals, and electrically insulated from the tube wall by means of a suitable insulating material. The fluid at the outlet of the test section, which was a mixture of water and steam, flowed to the condenser where steam was condensed and some subcooling was introduced. During its flow through the downcomer the water temperature was increased by means of a preliminary heater. The water was then directed to a flow meter, and then further preheating was made to the desired subcooled temperature just prior to the inlet side of the test section. The power input to the vertical preliminary heater and the setting of the valves were kept constant at all runs. Degasing was made by circulating the the coolant near saturation temperature with the main heater and pre-heaters switched on for about two hours.

3. EXPERIMENTAL PROCEDURE

3.1 Experimental Measurements :

During each run the following measurements were made :

(1) Temperature of the heating surface in the test section at nine equal intervals in the longitudinal direction.

(2) Water temperature at the inlet to the test section; and mixture temperature at the outlet of the test section.

(3) Water temperature at the condenser outlet.

(4) Coolant flow rate through the loop.

(5) Inlet power to the test-section.

(6) Inlet and outlet temperatures of the secondary coolant in the condenser.

(7) Flow rate of the secondary coolant in the condenser.

3.2 Methods of Experimental Calculations :

3.2.1 Exit steam quality :

The exit steam quality was calculated from

$$X_e = \frac{\frac{Q}{W} - C \left(T_{sat} - T_i \right)}{L} \tag{1}$$

Equation (1) was obtained from a heat balance in the test section. Heat losses to the atmosphere through the outside surface of the glass jacket, which were estimated and was found to be small, were ignored in the previous expression.

3.2.2 Boiling length :

The boiling length was calculated from

$$\ell_b = \frac{W L X_e}{Q} \tag{2}$$

According to equation (2) the boiling length represented the length of the test section at which nucleate boiling and other forms of advanced boiling regimes (plug, slug and annular two-phase flow patterns) happened. The length at which subcooled boiling occured was not included in the boiling length.

The non-boiling length ($\ell_{nb} = \ell - \ell_b$) might also be calculated from

$$\ell_{nb} = \frac{W C \left(T_{sat} - T_i \right)}{Q} \tag{3}$$

3.2.3 Local steam quality :

Since the heat generation was linear in the test section, the local steam quality varied also in a linear manner and was calculated from

$$X = \left(\frac{Z - \ell_{nb}'}{\ell_b}\right) X_e$$

$$= \left(\frac{Z - \ell_{nb}}{\ell}\right)\left(\frac{\ell}{W \, L}\right) \qquad \text{for } \ell_{nb} < Z < \ell_b \qquad (4)$$

3.2.4 Local heat transfer coefficient :

The local heat transfer coefficient at different points along the test section was calculated from the following expressions :

(1) **In the boiling region ($\ell_{nb} \leqslant Z \leqslant \ell$) :**

$$h = \frac{q}{T_w - T_{sat}} \qquad (5)$$

(2) **In the non-boiling region ($0 \leqslant Z \leqslant \ell_{nb}$) :**

The region might be divided into the following two sub-regions:

(a) **Single phase region :**

This is the region confined between the inlet of the test section and the point on the heater surface where the first nucleation site started nucleating. In this region the heat transfer coefficient was calculated from

$$h = \frac{q}{T_w - T_b} \qquad (6)$$

(b) **Sub-cooled boiling region :**

This is the region confined between the point on the heater surface where the first nucleation site started nucleating and the point where the bulk of liquid reached the saturation temperature.

Since the driving force in any boiling system is the temperature difference ($T_w - T_{sat}$), the heat transfer coefficient in this region is normally defined as in the boiling region by equation (5). However, at the beginning of this

region where the number of the nucleating sites is usually
small to affect the mechanism by which heat flows from the
heated solid surface to the bulk of liquid a definition for
the heat transfer coefficient as in the single phase region,
given by equation (6), might be more appropriate. Also
using equation (5) leads to discontinuity in the heat trans-
fer coefficient at the beginning of this region, since at
this point the heat transfer coefficient will be calculated
in the single phase region from equation (6) and in the
subcooled region from equation (5). The two expressions
will lead to two different values for the heat transfer
coefficient (h) since the bulk temperature (T_b) is less than
the saturation temperature (T_{sat}). Such discontinuity in
the heat transfer coefficient at that point, which is due to
different definitions, has no physical justification, and in
fact it does not exist. Moreover, at the end of this region,
where the heat transfer from the wall surface to the bulk of
liquid is mainly due to subcooled boiling, the bulk tempera-
ture is not much lower than the saturation temperature and
equations (5) and (6) lead almost to the same value of (h).
Because of this the heat transfer coefficient in the non-
boiling region was calculated in this analysis from equation
(6) and shown as full lines in Figs. (1) to (6). Additional
presentation of (h) in some of these figures, calculated from
equation (5), was shown as dotted lines. The start of sub-
cooled boiling was detected in the experiments by visual.
means.

3.3 Error Estimation in Experimental Results :

The temperatures of the heater surface measured by the embeded
thermocouples were corrected to take into account temperature drops
between the position of the thermocouples and the outer surface in
contact with the coolant.

The coolant flow rate measured by the flow meter was corrected to take into account density variations between calibration conditions at room temperature and actual experimental conditions near saturation temperature at atmospheric pressure.

Correction methods and a detailed error analysis are presented in $\underline{/\;2/}$. The maximum errors in the measured and the calculated parameters were estimated as :

Parameter	Maximum error ($\pm$)
power (Q)	3.48%
flow rate (W)	2.5%
exit steam quality (X_e)	15.0%
heat transfer coefficient (h)	10.0%
wall surface temperature (T_w)	0.855°C
coolant temperature (T)	0.612°C

The maximum percentage error in the exit steam quality corresponded to the case when the steam quality was low (i.e. low heat flux and high subcooling). As the heat flux was increased and the subcooling was decreased, the exit steam quality increased, and the estimated percentage error in it was lower than the prequoted value.

4. ANALYSIS OF EXPERIMENTAL RESULTS

4.1 Surface Temperature Distribution :

The surface temperature, the fluid bulk temperature, the heat transfer coefficient and the steam quality at different points along the test section are shown in Figs. (1) to (6) for a diameter ratio of the annular space equivalent to 2/1. For comparison, the curves in Figs. (1) to (3) are shown for different inlet temperatures of 91, 95 and 99°C at particular heat fluxes of 10.58, 16.75 and 20.9 watt/cm^2 respectively, and vice-versa for the curves shown in Figs. (4) to (6).

The curves show peculiar wall surface temperature and heat transfer coefficient distribution in the longitudinal direction of the flow especially at the inlet part of the test section. As an example, the wall surface temperature increased in Fig. (2) at the inlet in the flow direction when the inlet temperature and the wall heat flux were 91°C and 16.75 watt/cm^2 respectively. When the inlet temperature was increased to 99°C, the wall surface temperature at the inlet decreased in the flow direction for the same wall heat flux. Similar peculiar wall surface temperature distribution appeared also at the exit of the test section. In Figs. (4) to (6), the wall surface temperature indicated by the last thermocouple was higher than the temperature indicated by the two preceding ones. This noticable temperature rise at the outlet of the test section, which was observed in most two phase flow runs, was not present in the single phase flow runs as that shown in Fig. (7).

Before such temperature distribution can be explained, the different mechanisms by which heat flow from a heated surface to a boiling liquid in a flow channel are briefly reviewed. End effects, which modify the temperature at the inlet and outlet of the channel, are ignored at first then analysed separately. The temperature distribution at the entrance and outlet of the channel is dependant on the combined contribution of end effects as well as the other heat transfer mechanisms.

4.1.1 Heat transfer from a uniformly heated surface to a boiling liquid (end effects ignored) :

The heat transfer coefficient from a uniformly heated surface placed in a long vertical channel to a fluid varies in the direction of the flow as the fluid varies from the pure liquid phase at the inlet to the pure vapour phase at the outlet of the channel. Such heat transfer coefficient distribution is shown in Fig. (8). The different regions, presented in this figure will here-after be briefly discussed :

Region (1) :

In this region, only subcooled liquid is present in the channel. The mechanism of heat transfer is by single phase convection. The heat transfer coefficient is almost uniform, the slight rise in its value in the flow direction is due to change in physical properties of the liquid as the bulk and wall surface temperature increase.

Region (2) :

This is the subcooled boiling region. In this region vapour bubbles, which are formed in a thin superheated layer near the heated solid surface, collapse as they move far from the solid surface in the bulk of liquid. At the beginning of this region the number of the nucleating sites is small to affect the mechanism of heat transfer, and the heat transfer coefficient is that of a single phase flow as in region (1). At the end of this region the bubble population increases considerably, and their growth and collapse become very effective in modifying the value of the heat transfer coefficient which approaches that value of nucleate boiling in region (3).

Region (3) :

This is the nucleate boiling region. It begins at the point where the bulk temperature reaches the saturation temperature. The heat transfer coefficient is high and almost uniform. The two phase flow present in that region is sometimes called "bubble flow".

Region (4) :

In this region, vapour bubbles accumulate and coalesce at the core of the channel forming what is sometimes called "plug, slug and annular flow". The change from plug to slug and finally annular flow happens in the direction of the flow as more vapour accumulates in the channel core. The important feature of that region is the presence of a thin film of liquid surrounding the heated surface. The thickness of the film decreases in the flow direction causing a continuous increase in the heat transfer coefficient.

Region (5) :

This region starts when the liquid film vanishes by evaporation and vapour comes in contact with the heated surface. A sudden drop of the heat transfer coefficient happens, followed by a more flat distribution. In this region liquid drops are distributed in the vapour space. The point at which the heat transfer coefficient suddenly drops is known as burn out "or dry out". The surface temperature rises considerably in that region, and in some cases damage to the heating surface happens either by melting or distortion of the heating element.

Region (6) :

This is the region of superheated vapour. It starts at the point where the liquid drops, present in the vapour, disappear. At that point the vapour is just saturated. The mechanism of heat transfer is by single phase convection. The heat transfer coefficient is generally lower than the corresponding heat transfer coefficient in the liquid phase at the beginning of that region, but it approaches it and might exceed it as the vapour is further superheated.

Dividing the flow pattern to the previous regions is very general in nature. Main Parameters (e.g. heat flux and mass flow rate, etc...) might have a considerable effect in modifying the regions. For example, for the same mass velocity burn out might happen at an earlier stage than in region (4) if the heat flux is increased beyond a certain limit.

The first four regions were generally present along the heater length in the experimental work. Their position and hence their contribution depended on the level of heat flux and inlet temperature to the test section. The last regions were not present, in fact the combination wall heat flux and inlet temperature were regulated to avoid heater damage by burn out.

For simple analysis, the heat transfer coefficient in each of the four first regions may be approximated by a linear distribution in the

flow direction as shown in Fig. (9). In region (1) and (3) the heat transfer coefficient is assumed constant. The film temperature drop corresponding to the heat transfer coefficient distribution, and the bulk temperature of the coolant are shown also in Fig. (9). The bulk temperature in regions (3) and (4) is the saturation temperature corresponding to the system pressure, the drop in its value due to pressure drop along the channel length is ignored.

The heat transfer coefficient can now be expressed in the different regions by the following relations :

Region (1) :

$$h_c = \text{constant} \tag{7}$$

Region (2) :

$$h_s = h_c + \left(\frac{h_n - h_c}{\ell_s}\right) Z_s \tag{8}$$

Region (3) :

$$h_n = \text{constant} \tag{9}$$

Region (4) :

$$h_{\ell f} = h_n + \left(\frac{h_{\ell fm} - h_n}{\ell_{\ell f}}\right) Z_{\ell f} \tag{10}$$

The bulk coolant temperature is given by :

Region (1) :

$$T_b = T_i + \frac{q_s Z_c}{W c} \tag{11}$$

Region (2) :

$$T_b = T_i + \frac{q_s (\ell_c + Z_s)}{W c} \tag{12}$$

Region (3) :

$$T_b = T_{sat} \tag{13}$$

Region (4) :

$$T_b = T_{sat} \tag{14}$$

The wall surface temperature is, then, given by :

Region (1) :

$$T_w = T_b + \frac{q}{h_c}$$

$$= \left[T_i + \frac{q}{h_c}\right] + \left(\frac{q\ s}{W\ c}\right) Z_c \tag{15}$$

for $0 \leqslant Z_c \leqslant \ell_c$

Region (2) :

$$T_w = T_i + \frac{q\ s(\ell_c + Z_s)}{W\ c} + \frac{q}{h_c + \left(\dfrac{h_n - h_c}{\ell_s}\right) Z_s}$$

$$= \left[T_i + \frac{q\ s\ \ell_c}{W\ c}\right] + \frac{q\ s\ Z_s}{W\ c} + \frac{q}{h_c + \left(\dfrac{h_n - h_c}{\ell_s}\right) Z_s} \tag{16}$$

for $0 \leqslant Z_s \leqslant \ell_s$

Region (3) :

$$T_w = T_{sat} + \frac{q}{h_n} \tag{17}$$

for $0 \leqslant Z_n \leqslant \ell_n$

Region (4) :

$$T_w = T_{sat} + \frac{q}{h_n + \left(\dfrac{h_{\ell fm} - h_n}{\ell_{\ell f}}\right) Z_{\ell f}} \tag{18}$$

for $\quad 0 \leqslant Z_{\ell f} \leqslant \ell_{\ell f}$

From the previous equations, it is clear that the wall surface temperature increases linearly in region (1), constant in region (3) and decreases linearly in region (4). However, the wall surface temperature distribution in region (2) is more complicated. The second term in equation (16) increases while the third term decreases in the flow direction. The expression might have a minimum. To obtain the point of minimum wall surface temperature, equation (16) is differentiated with respect to Z_s, and the derivative is equated to zero, or

$$\frac{d\,T_w}{d\,Z_s} = \frac{q\,s}{W\,c} - \frac{q\,(\frac{h_n - h_c}{\ell_s})}{\left[h_c + (\frac{h_n - h_c}{\ell_s})\,Z_s \right]^2} \tag{19}$$

if Z_{sm} corresponds to the point of minimum wall surface temperature, then

$$\frac{s}{W\,c} - \frac{(\frac{h_n - h_c}{\ell_s})}{\left[h_c + (\frac{h_n - h_c}{\ell_s})\,Z_{sm} \right]^2} = 0 \tag{20}$$

Re-arranging gives

$$Z_{sm} = \pm \left[\frac{W\,c\,\ell_s}{s\,(h_n - h_c)} \right]^{\frac{1}{2}} - \frac{h_c\,\ell_s}{(h_n - h_c)} \tag{21}$$

The negative sign before the square root in equation (21) can be ignored since it has no physical meaning, or

$$\frac{Z_{sm}}{\ell_s} = \left[\frac{W\,c}{s\,\ell_s\,(h_n - h_c)} \right]^{\frac{1}{2}} - \frac{h_c}{h_n - h_c} \tag{22}$$

To insure that the wall surface temperature achieves a minimum, the second derivative of T_w with respect to Z_s is obtained, or

$$\frac{d^2 T_w}{d Z_s^2} = + \frac{2 q \left(\dfrac{h_n - h_c}{\ell_s}\right)^2}{\left[h_c + \left(\dfrac{h_n - h_c}{\ell_s}\right) Z_s \right]^3} \qquad (23)$$

Since $\left(h_n - h_c \right) > 0$,

hence $\left(d^2 T_w / d Z_s^2 \right)$ is positive for all positive or zero values of $\left(Z_s \right)$, and the wall surface temperature achieves a minimum, rather than a maximum, in the subcooled region. However, in order that a minimum is achieved in that region, the value of $\left(Z_{sm} \right)$ obtained from equation (21) must lie within the following limits.

$$0 \leqslant Z_{sm} \leqslant \ell_s$$

or

$$0 \leqslant \frac{Z_{sm}}{\ell_s} \leqslant 1$$

If the ratio $\left(Z_{sm} / \ell_s \right)$ lies outside the previous range, the point of minimum wall surface temperature lies outside the subcooled region where the method of calculations is not valid.

Thus, if

$$\left[\frac{W c}{s \, \ell_s \, (h_n - h_c)} \right]^{\frac{1}{2}} - \frac{h_c}{h_n - h_c} < 0$$

then $Z_{sm} < 0$, and the wall surface temperature distribution in the subcooled region shows a continuous rise as shown in Fig. (10a).

Also, if

$$\left[\frac{W c}{s \, \ell_s \, (h_n - h_c)} \right]^{\frac{1}{2}} - \frac{h_c}{h_n - h_c} > 1$$

then $Z_{sm} > \ell_s$, and the wall surface temperature shows a continuous decrease in the subcooled region as shown in Fig. (10b).

The two special cases when $\bar{z}_s = 0$ or ℓ_s are shown in Figs. (10c) and (10d) respectively.

The previous analysis is applied to one of the experimental runs as follows :

Parameters of the experiment :

inlet temperature (T_i) = 91°C

wall heat flux (q) = 10.58 watt/cm^2

diameter ratio (D_o/D_i) = 2/1

Data obtained from the experiment :

flow rate (W) = 47.5 gram/sec.

velocity in test section (V) = 20 cm/sec.

convection length (ℓ_c) = 10 cm

subcooling length (ℓ_s) = 60 cm

The convection length was estimated visually (i.e. the length from the inlet to the point where the first bubble appeared on the heating surface). However, methods similar to those presented in $\underline{/}3\underline{/}$ may be used to predict the point of boiling incipience.

The heat transfer coefficient in the convection region, in case of absence of end effects, may be calculated from the correlation $\underline{/}4\underline{/}$

$$N_u = 0.00131 \, (R_e)^{1.065} \, (P_r)^{0.40} \, (\frac{D_o}{D_i})^{0.55} \tag{24}$$

The previous correlation is recomended for the case of annular flow with diameter ratios from 1.5 to 2.0 and for Reynolds numbers in the transition region from 2×10^3 to 1×10^4.

Now,

equivalent diameter (D_e) $= D_o - D_i$

$= 2/1$

$= 1 \text{ cm}$

Reynolds number (R_e) $= \dfrac{V D_e}{u_\ell}$

$= \dfrac{20 \times 1 \times 0.97}{3 \times 10^{-3}}$

$= 6.5 \times 10^3$

Prandtl number (P_r) $= 2 \text{ (at } 91\degree C)$

Thus, from equation (24),

Nusselt number (N_u) $= 29.2$

and

$$h_c = \dfrac{N_u K}{D_e}$$

$$= \dfrac{29.2 \times 6.8 \times 10^{-3}}{1}$$

$$= 0.2 \text{ watt/cm}^2 \degree C$$

The heat transfer coefficient in the nucleate region was determined experimentally from measurements of the wall surface temperature and the liquid bulk temperature in that region (last thermocouple reading, where end effects were present, was excluded). This gave

$$h_n = 0.7 \text{ watt/cm}^2 \degree C$$

Thus, from equation (16),

$$T_w = \left(91 + \dfrac{10.58 \times 3.14 \times 10}{47.5 \times 4.2}\right) + \left(\dfrac{10.58 \times 3.14 \times Z_s}{47.5 \times 4.2}\right)$$

$$+ \left(\dfrac{10.58}{0.2 + \left(\dfrac{0.7 - 0.2}{60}\right) Z_s}\right)$$

$$= 92.7 + 0.167 Z_s + \dfrac{10.58}{0.2 + 0.00833 Z_s}$$

The point of minimum wall surface temperature (Z_{zm}) is given by

$$\frac{Z_{zm}}{l_s} = \left[\frac{47.5 \times 4.2}{3.14 \times 60 \times (0.7 - 0.2)}\right]^{\frac{1}{2}} - \left[\frac{0.2}{0.7 - 0.2}\right] = 1.05$$

or the wall surface temperature continues to decrease till the end of the subcooled region.

The wall surface temperature in the subcooled region according to this calculation is shown in Fig. (11). The experimental points are also plotted. On the same figure. It is seen in that figure that, except at the beginning of that region where entrance effects were still present, there is a fair agreement between experimental and calculated distribution.

Similar temperature distribution patterns were observed at other runs. In all cases temperature decrease in the longitudinal direction was observed in the subcooled region (outside the entrance length).

In the region of nucleate boiling the wall surface temperature was uniform, or the heat transfer coefficient was constant. This agrees with previous findings of other workers $\underline{/5/}$.

In the runs in which the heat flux was high and the subcooling was low (e.g. Fig. (5), for $q_w = 20.9$ watt/cm^2), there was a chance for a region to develop at the end of the test section where a slug flow was present. Temperature distribution in such regions showed a tendency towards a decreasing wall surface temperature in the direction of the flow. Thus was, as previously explained, due to the increased heat transfer coefficient as the liquid film thickness decreased. However, the last thermocouple showed a temperature rise in most runs, this was attributed to end effects and will be discussed later.

In the convection region at the inlet of the test section as well as a part of the subcooled region (in most runs) the temperature distribution was influenced by entrance effects, which were superimposed

on the original temperature distribution that would have been present
if these effects were not there.

4.1.2 End effects :

(1) Effect at the inlet of test section :

There are two main effects which had a considerable influence
on the temperature distribution of the heated surface at the
inlet of the test section. These are :

(a) Temperature and velocity profiles at inlet :

It is well known that in a uniformly heated channel,
where there is no change of phase, a high heat transfer co-
efficient is achieved at the point where heating starts,
followed by a continuous reduction in its magnitude for a
certain length known as the "entry length". After this
length, the heat transfer coefficient becomes uniform as
shown in Fig. (12). The theoretical value of the heat trans-
fer coefficient at the point where the heat flux is applied
is infinite : However, because of some conduction in the
wall in a direction opposite to the direction of the flow,
which is inevitable, a thermal layer develops earlier to
that point and the heat transfer coefficient achieves a
high, but finite, value.

Such heat transfer coefficient distribution can be fur-
ther enhanced if heating starts at the inlet of the channel,
where the velocity distribution is uniform across the entire
flow area. The developing of a laminar layer near the solid
heated surface increases the resistance to heat flow in the
direction of fluid flow. After a certain length, the laminar
layer becomes fully developed and the resistance to heat
flow becomes uniform.

The combined effects lead to reduction in the wall sur-
face temperature in the direction of the flow in the entrance

region. This is shown in the single phase run presented in Fig. (7).
An entrance length between 20 to 30 equivalent diameters $(D_e = 1 \text{ cm})$
was required in Fig. (7) before the heat transfer coefficient achieved
its uniform value. The continuous nearly linear rise in the heat
transfer coefficient after the entrance length is due to variations
in the physical properties (mainly viscosity).

It is expected in the boiling runs that, as the inlet subcooling
was increased and/or the wall heat flux was decreased the length of the
convection region increased. Entrance effects were important at the
inlet, and the first thermocouple indicated in those runs a wall sur-
face temperature much lower than the second and third ones. As the
inlet subcooling was decreased and the wall heat flux was increased
the length of the convection region decreased. When this was continued
further, subcooled boiling started nearly from the beginning; thus
eliminating the convection region. Now, two mechanisms worked at the
inlet, which opposed at the same time one another. As the coolant
proceeded along the test section in the flow direction, the heat trans-
fer coefficient tended to decrease by virtue of entrance effects, but
at the same time more sites nucleated and subcooled boiling became
more pronounced leading to an increase in the heat transfer coefficient
in the flow direction. The resultant effective heat transfer coeffi-
cient is due to the combined effects of the two mechanisms. At high
subcooling and/or low wall heat flux the entrance effects became more
dominant at the inlet and the wall surface temperature increased in
the direction of the flow (e.g. Fig. (1), at 91°C inlet temperature).
On the other hand at low subcooling and/or high heat flux subcooled
boiling became more dominant and the wall surface temperature decreased
in the flow direction (e.g. Fig. (3), at 99°C inlet temperature). Some-
where in between the two effects counter-balanced one another, and the
temperature distribution at the inlet became nearly uniform as seen in
Fig. (6).

(b) <u>Conduction in the solid wall</u> :

The two ends of the heater were screwed to thick brass
tubes, which in turn were fixed to heavy copper bus-bars.
These bars worked as a cold sink and some conduction from
the hot heater to the relatively colder bus-bars was inevit-
able. The upper brass tube at the outlet of the test sec-
tion was partly in contact with mixture of steam and water
leaving the test section in the two phase runs. The tempera-
ture of that brass end was kept virtually constant and
equal to the saturation temperature of the coolant corres-
ponding to its pressure at the exit. This reduced conduction
in the heater tube in the flow direction at the outlet. The
situation was different at the inlet end. The brass tube
was surrounded by a small volume of stagnant water, which
was at an average temperature lower than the inlet tempera-
ture of the circulating coolant.

Thus, some conduction through the heater tube
happened at the inlet side opposite to the direction of the
flow, and the surface temperature measured by the first
thermocouple might have indicated a lower temperature than
what would have been indicated if conduction in that direc-
tion was not present.

(2) <u>Effect at the outlet of the test section</u> :

The temperature at the outlet of the test section, indicated
by the last thermocouple, was higher than that indicated by
the preceding two ones in most runs. This behaviour might
be explained by the following :

Near the outlet of the test section some of the vapour
bubbles coalesced and formed vapour plugs followed by vapour
slugs and finally an annular flow might have been present.
That all these flow patterns existed before the coolant left

the test section, or only some of them, depended on the level
of heat flux and inlet temperature. In such flow pattern a
thin film of liquid was present between the vapour and the
heating surface, the thickness of the film decreased in the
flow direction. At the outlet of the test section the vapour
(e.g. vapour slugs) followed the stream lines of the flow,
as shown in Fig. (13). Because of the geometry at the outlet
end, a thicker film thickness was present and the resistance
to heat flow became greater causing a rise in the wall sur-
face temperature. These arguments were supported by the fact,
that in the single phase flow runs such temperature rise was
not observed at the outlet (see Fig. (7)). Also in the two
phase runs, when the inlet temperature and the wall heat flux
did not allow the formation of vapour plugs and slugs, the
temperature rise at the outlet was either not present or,
negligable as seen in Fig. (14).

4.2   Coolant Mass Flow Rate :

The mass flow rate of the coolant is shown in Figs. (15) and (16)
against the heat input and the inlet coolant temperature respectively.
It is seen in Fig. (15) that at low heat inputs the rate of increase
of the mass flow rate with increase in power level was greater than at
high inputs. In other words, when the heat input exceeded a certain
value the coolant mass flow rate approached an asymptotic value. Such
limiting value was reached at lower heat input when the inlet tempera-
ture was high and vice-versa.

In Fig. (16), it is seen that the rate of increase of coolant mass
flow rate which increase in coolant temperature was low at low inlet
temperatures. However, this rate increased as the inlet temperature
was increased, and then decreased when the inlet temperature approached
the saturation temperature.

The behaviour of the coolant mass flow rate with both power and

inlet temperature, as seen in Figs. (15) and (16), might be explained
as follows :

The driving potential causing fluid circulation through the loop
was the difference in the average densities $(\rho_{md} - \rho_{mt})$ between the
relatively colder downcomer and the hotter test section. When the
heat input was small such that there was no boiling in the test sec-
tion, the average density (ρ_{mt}) was not much lower than that in the
downcomer (ρ_{md}), the difference was only due to thermal expansion of
the liquid in the single phase. However, when there was net boiling
in the test section the average density there decreased considerably
below the average density in the downcomer due to void formation in
the annular space of the test section. In the appendix a relation is
given between the steam volume fraction (α) and the steam quality (X)
for a flow of a mixture of steam and water at atmospheric pressure,
this relation is plotted in Fig. (17). It is seen in that figure that
at very low values of steam quality, the rate of increase of the steam
volume fraction with respect to steam quality is very high, as the
steam quality increases beyond a certain value $(say X > 0.03)$, which
is still small, the change of the volume fraction with respect to
quality becomes very small. At such steam qualities the channel is
almost full of vapour.

The steam quality at the outlet of the test section depended on
the heat input and the inlet temperature. For a particular inlet
temperature, the steam quality at the outlet increased as the power
was increased, hence the exit void fraction and the void fraction
averaged in the test section increased also. At low power level the
steam quality at the exit was very low and the rate of increase of the
average void fraction was high leading to high rate of increase of
density difference $(\rho_{md} - \rho_{mt})$ with respect to power increase. As
the power was increased further, a situation was reached in which the
vapour content in the test section was very high that further increase
in power has no appreciable effect on the density difference $(\rho_{md} - \rho_{mt})$

Similar behaviour is expected also with respect to temperature variations. At low inlet temperature (high subcooling), no net boiling was present. The density difference $(\rho_{md} - \rho_{mt})$ was only due to thermal expansion of the water, its rate of increase, and hence the rate of increase of coolant mass flow rate, with respect to increase in temperature was low. As the inlet temperature was increased to the level which initiated net boiling in the test section, the rate of increase of the density difference with increase in inlet temperature became high. This continued until the steam volume fraction became high, further increase in the inlet temperature showed no appreciable effect on the mass flow rate.

According to the previous arguments, it would be expected that the rate of increase of mass flow rate with increase in power would also be low when there is no net boiling in the test section. Such low level of power was not reached in the experiments, and hence was not plotted in Fig. (15).

4.3 Steam Quality :

The steam quality at the exit as a function of the power input presented in Fig. (18), was calculated from equation (1). It is clear from equation (1) that, if the coolant mass flow rate was constant, the exit steam quality would have been linearly dependant on the power. Since the coolant mass flow itself was a function of the power input, the relation between exit steam quality and power will not be linear. However, in the range of inlet temperature and power input, where the mass flow rate was less sensitive to inlet temperature and power variation, the relation between exit steam quality and power input may be approximated by a linear relation.

4.4 Diameter Ratio :

The effect of the diameter ratio on the coolant mass flow rate is shown in Fig. (19) at different wall heat fluxes and inlet temperatures. It is seen that there is a maximum value for the coolant flow rate

between the two limiting values of diameter ratio in all cases presented in Fig. (19). A possible explanation of this behaviour might be as follows :

As the diameter ratio of the annular space of the test section of a similar loop increases the inlet velocity decreases if the coolant mass flow rate is kept constant. Experiments showed that as the inlet velocity decreases the slip ratio increases $\underline{/5}$. From equation (A-2) in the appendix it appears that for the same exit quality, which will be the case if the power input and mass flow rate are kept constant, the exit void fraction decreases as the slip ratio increases; this results in a lower average steam volume fraction and hence a lower density difference. Thus, the trend is that the coolant mass flow rate decreases as the diameter ratio increases. However, the actual level of the coolant mass flow rate depends not only on the driving force (density difference) but also on the hydraulic resistance of the circuit. Increasing the diameter ratio increases the equivalent diameter and hence reduce the resistance to the flow. These two contradicting factors might lead to a maximum coolant flow rate between a certain range of diameter ratios. However, that these factors were responsible for the experimental behaviour cannot be emphasized before detailed calculations are made.

The effect of the diameter ratio on the heat transfer coefficient and hence the wall surface temperature was mainly in the entrance region. The entrance length varied considerably from one diameter ratio to another. The coolant mass flow rate, which varied from one diameter ratio to another, might have had a small effect on the heat transfer coefficient at the region of relatively high steam quality near the exit of the test section.

The flow pattern at the outlet of the test section varied according to the diameter ratio. A high diameter ratio led to less bending of the stream lines, and hence less bending of the vapour slugs. This might explain, why the last thermocouple did not show higher temperature

than the preceding ones at the high diameter ratio. The wall surface temperature distribution at different diameter ratios for a particular value of inlet temperature and of wall heat flux is shown in Fig. (20).
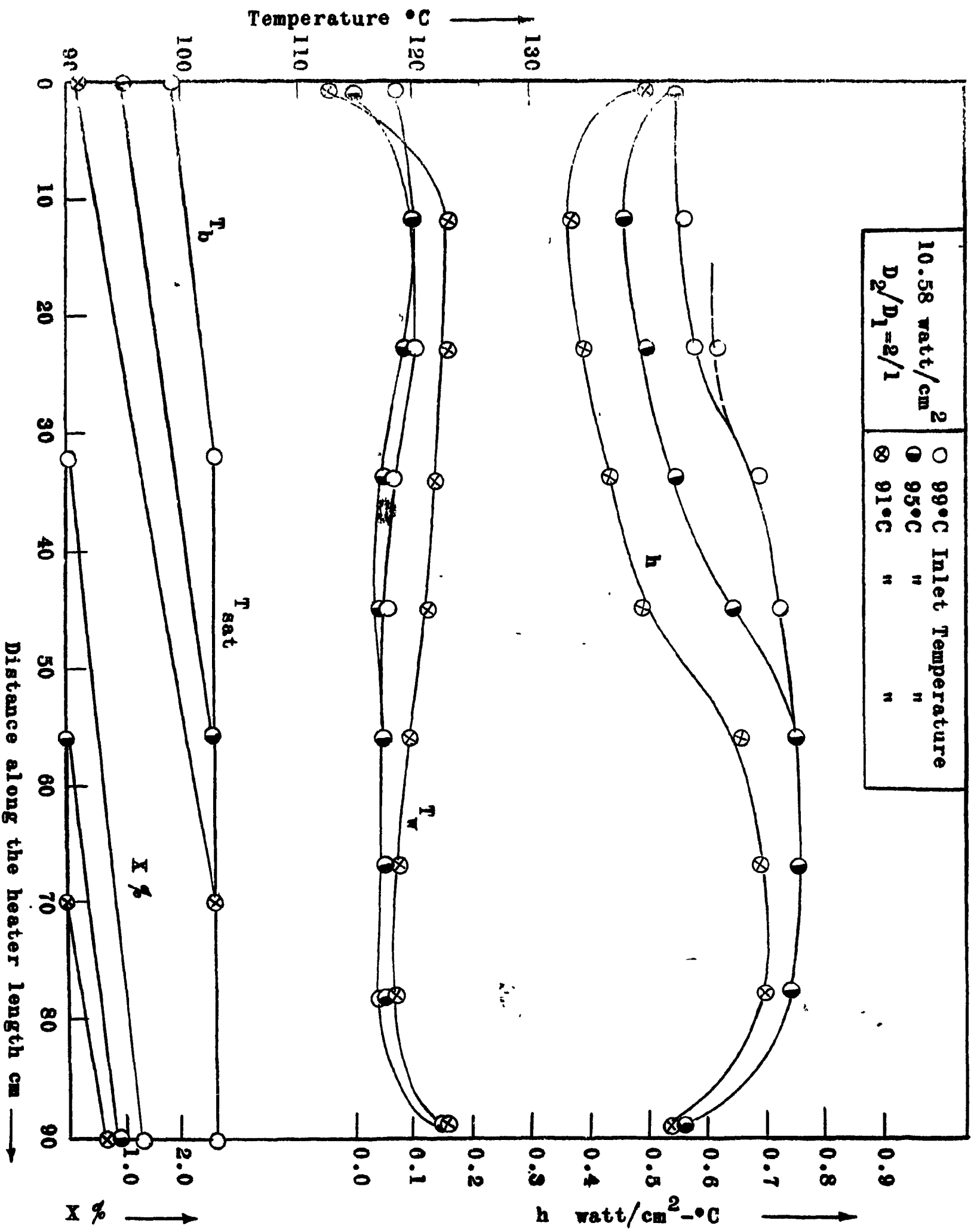
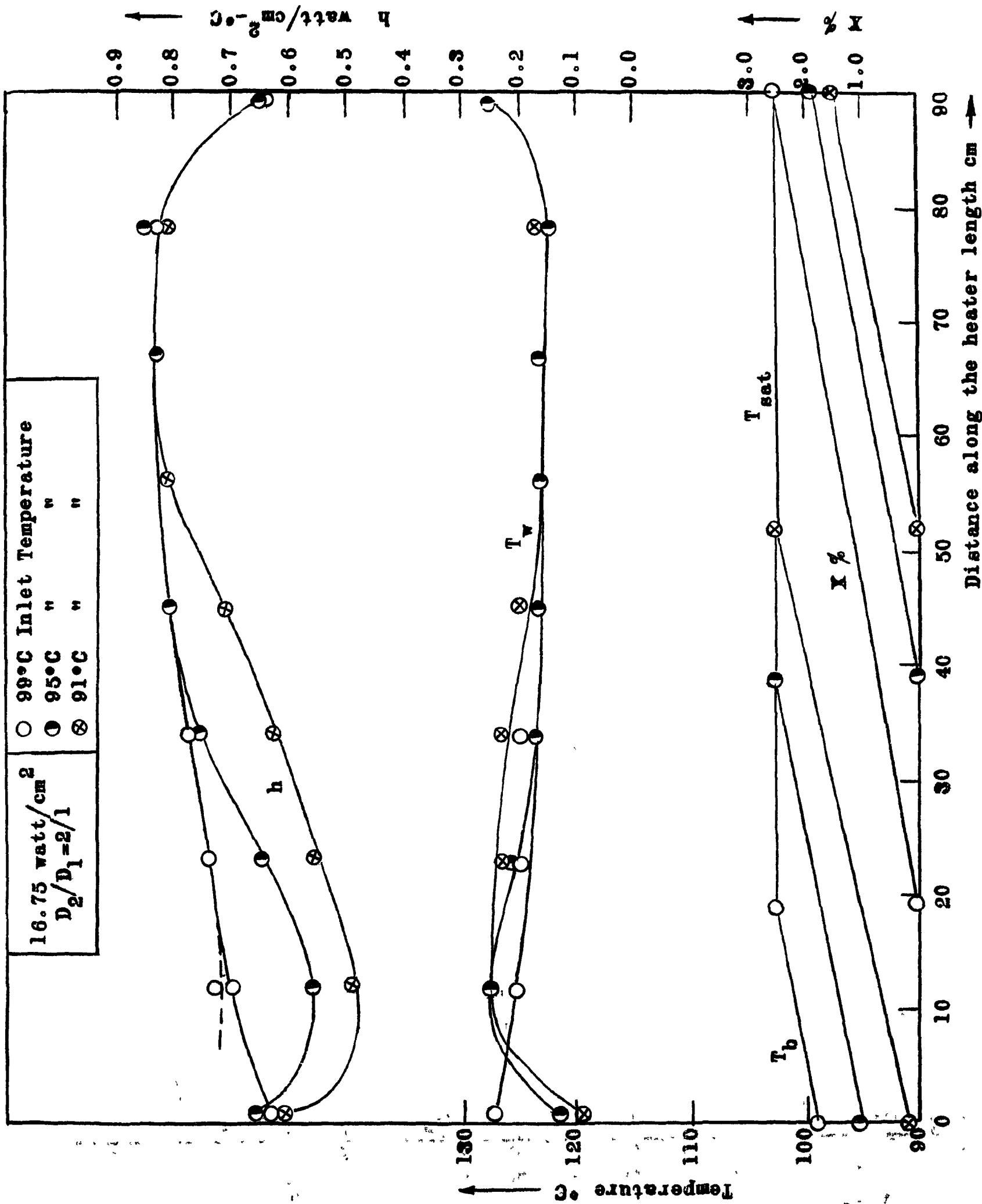Fig. (1): Experimental Runs at 10.58 watt/cm².
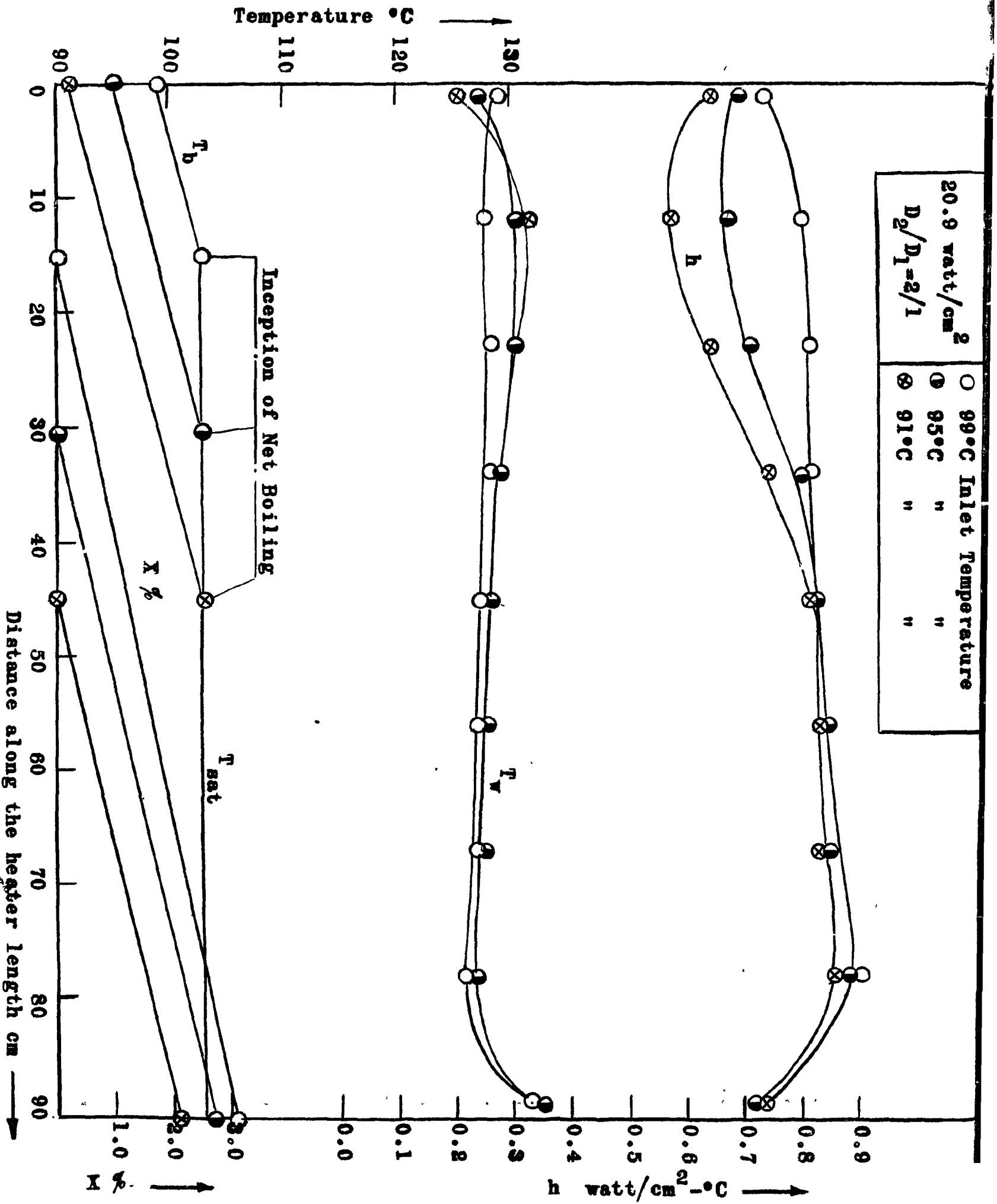
Fig. (2): Experimental Runs at 16.75 watt/cm².
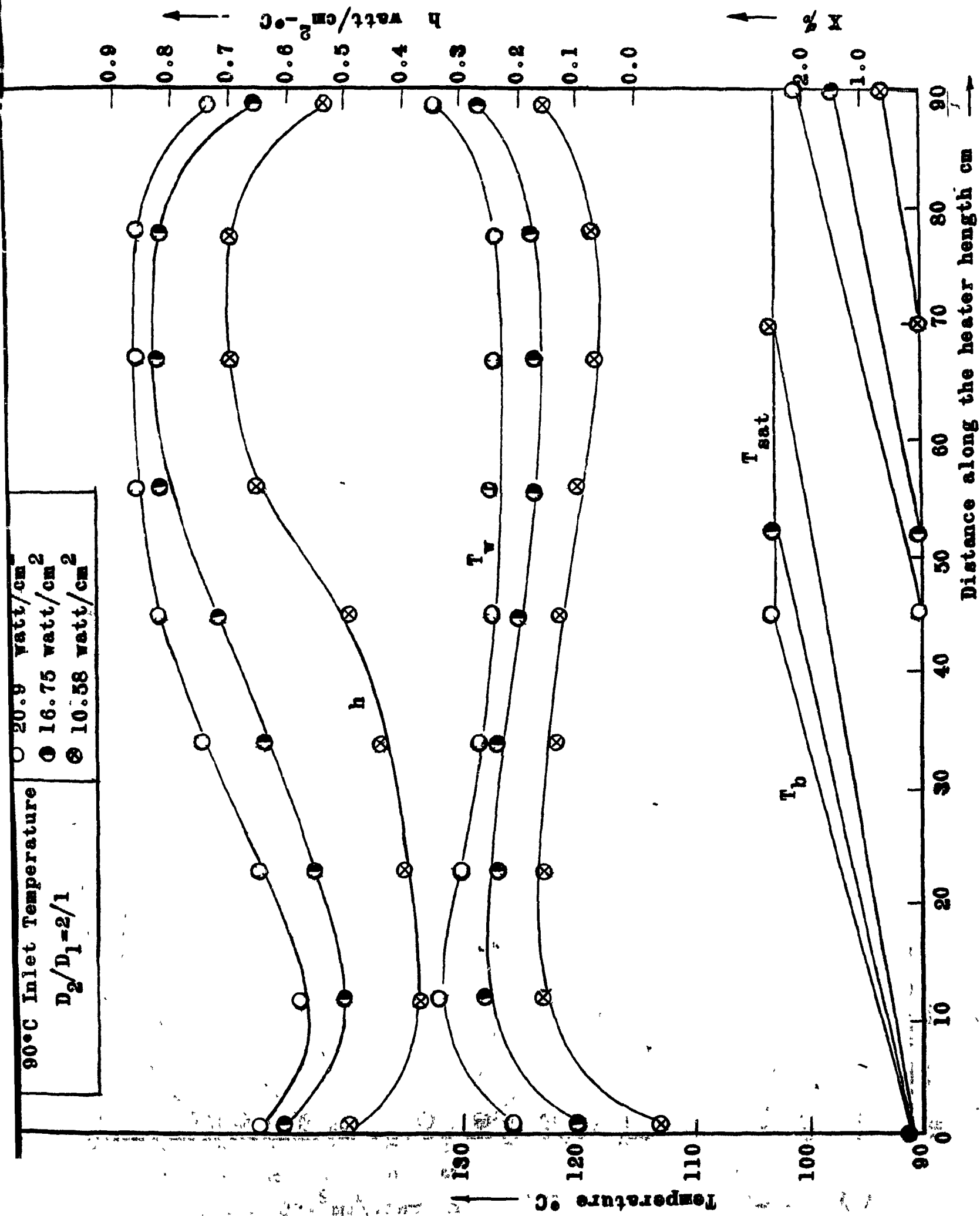
Fig. (3): Experimental Runs at 20.9 watt/cm².
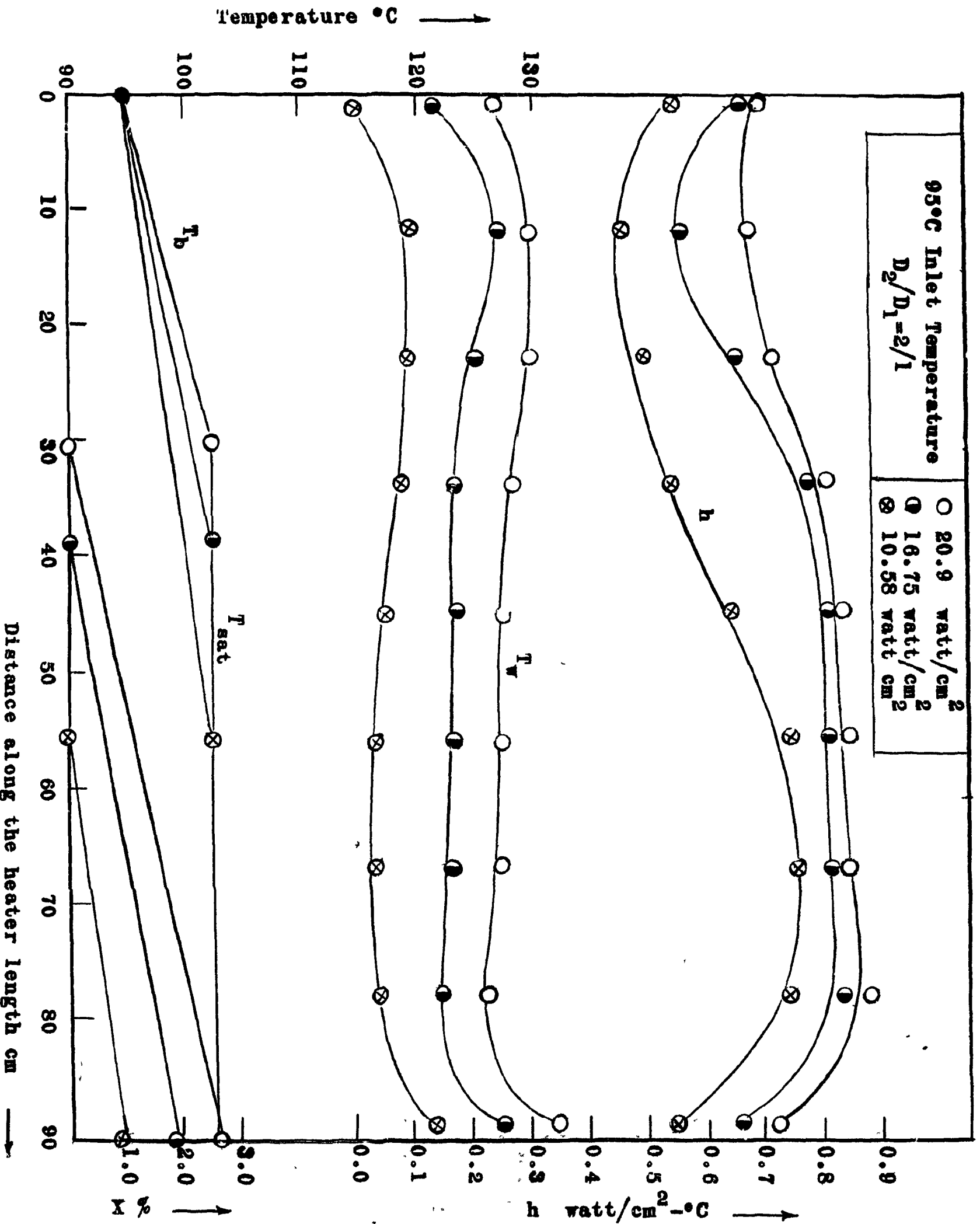
Fig. (4): Experimental Runs at 91°C Inlet Temperature.
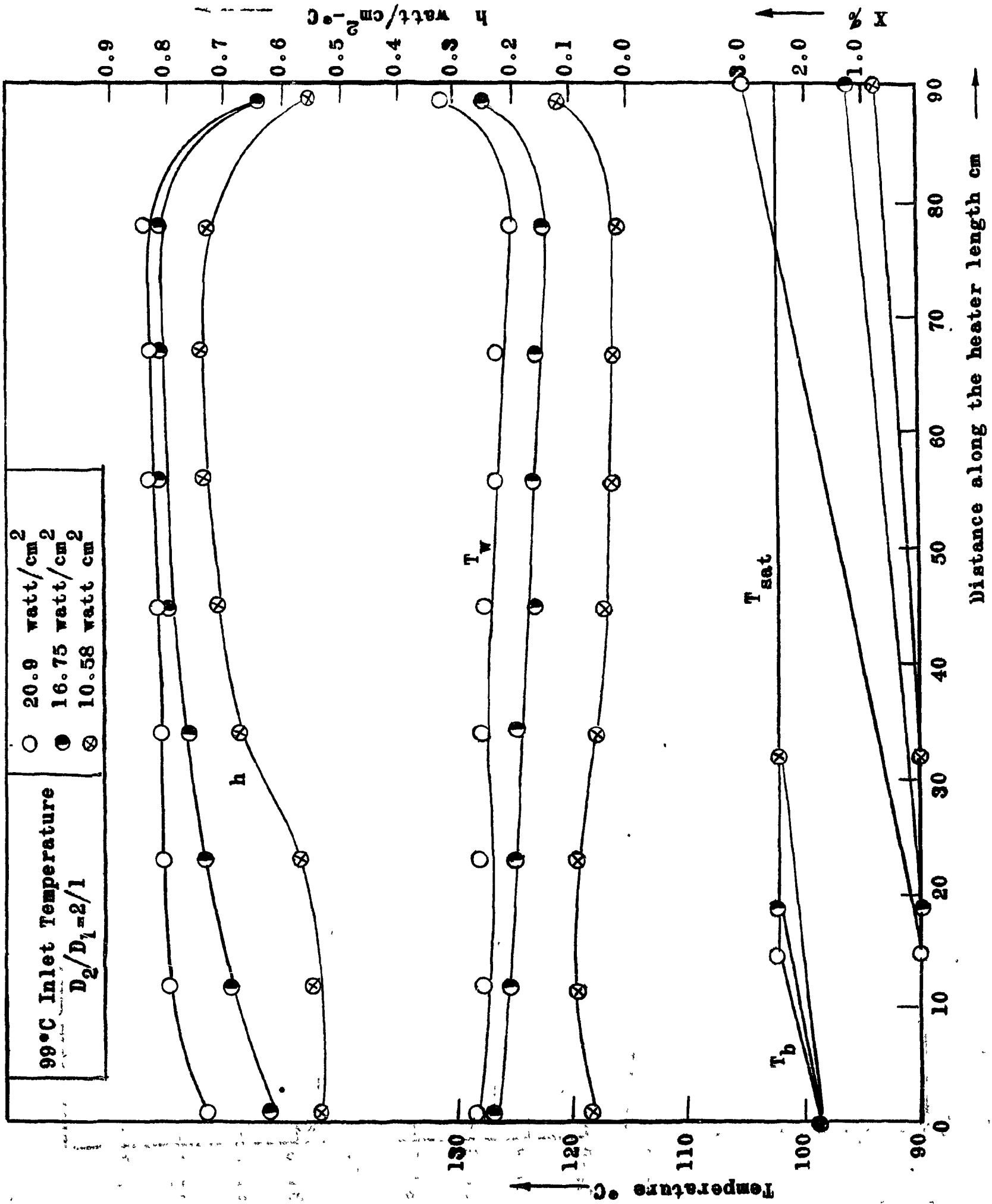
Fig. (5): Experimental Runs at 95°C Inlet Temperature.

Fig. (6): Experimental Runs at 99°C Inlet Temperature.
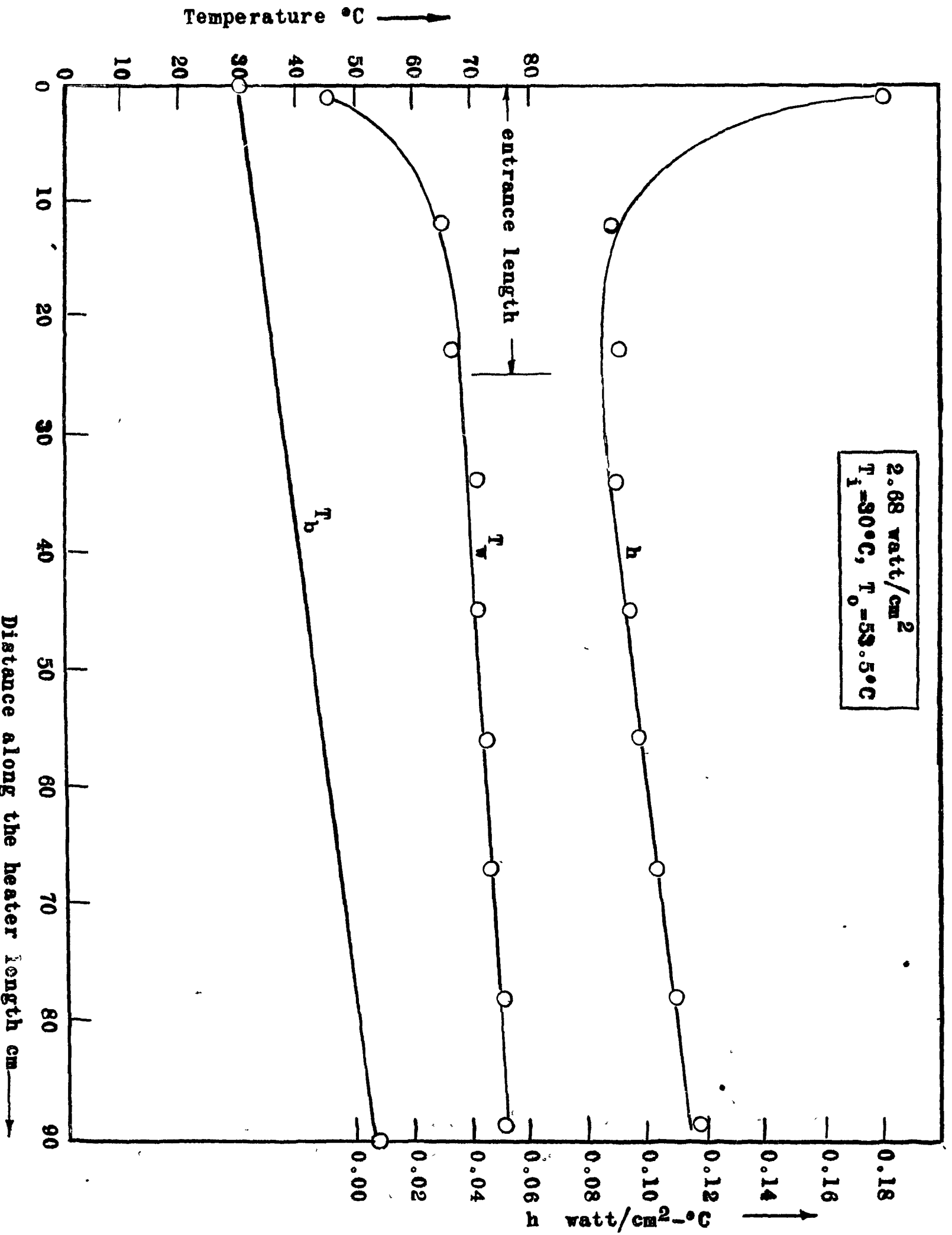
Fig. (7): Single Phase Flow Run at 2.68 watt/cm².

Region 1 — single phase convection (liquid phase)	Region 2 — subcooled boiling	Region 3 — Nucleate boiling	Region 4 — film of liquid boiling	Region 5 — burn out	Region 6 — single phase convection (gas phase)

saturated liquid · · · · · · · · · · saturated vapour

channel length →

pure liquid (subcooled)	liquid + vapour bubbles near the heated surface	liquid + vapour bubbles bubble flow	mainly vapour in the core with dispersed liquid drops + liquid film near the solid surface (plug, slug or annular dispersed flow)	vapour + dispersed liquid drops	pure vapour (super-heated)

flow → direction

Fig. (8): Heat Transfer Coefficient Distribution along the Channel Length.
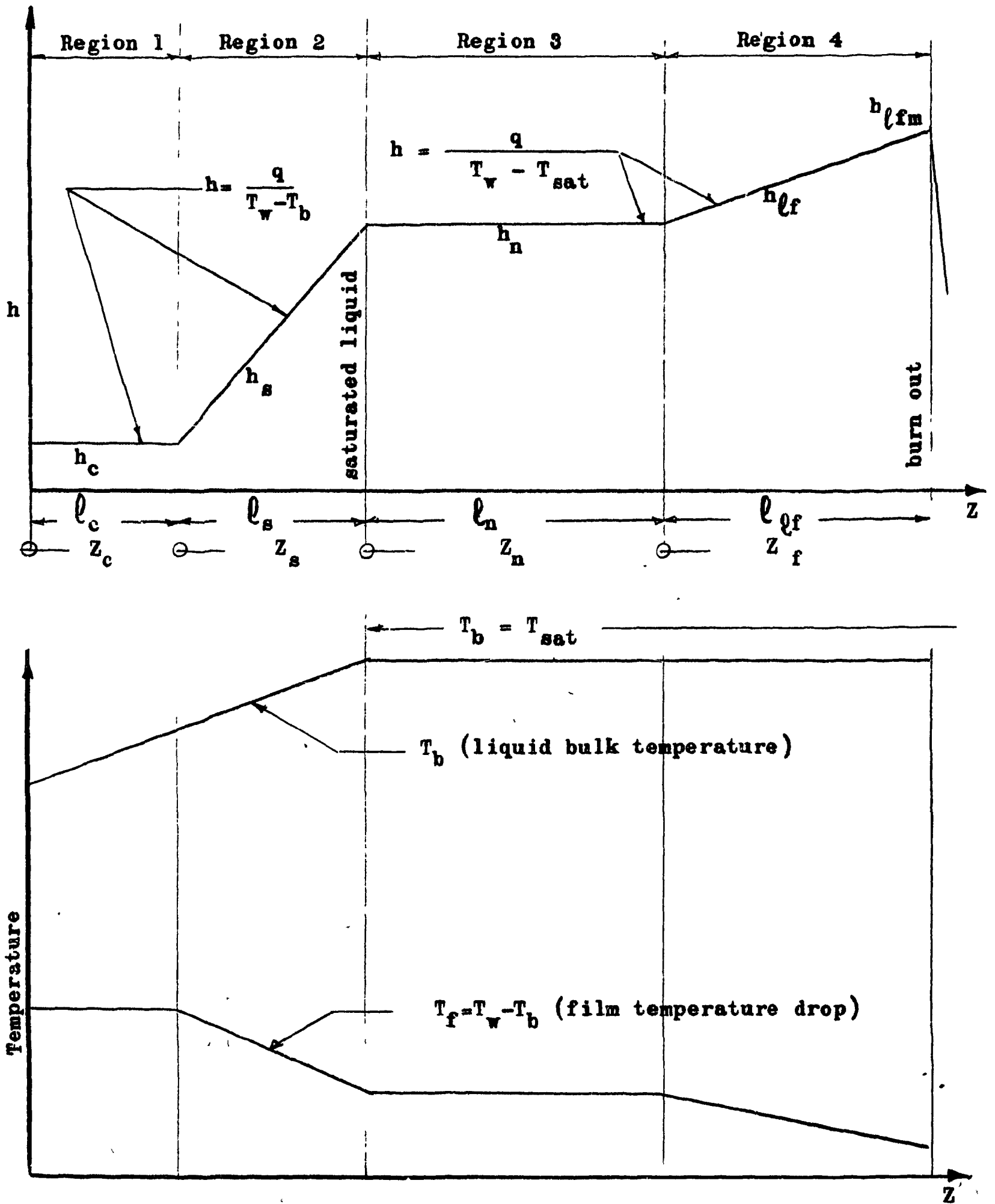
Fig. (9): Heat Transfer Coefficient, Bulk Temperature and Film Temperature Drop along The Channel.
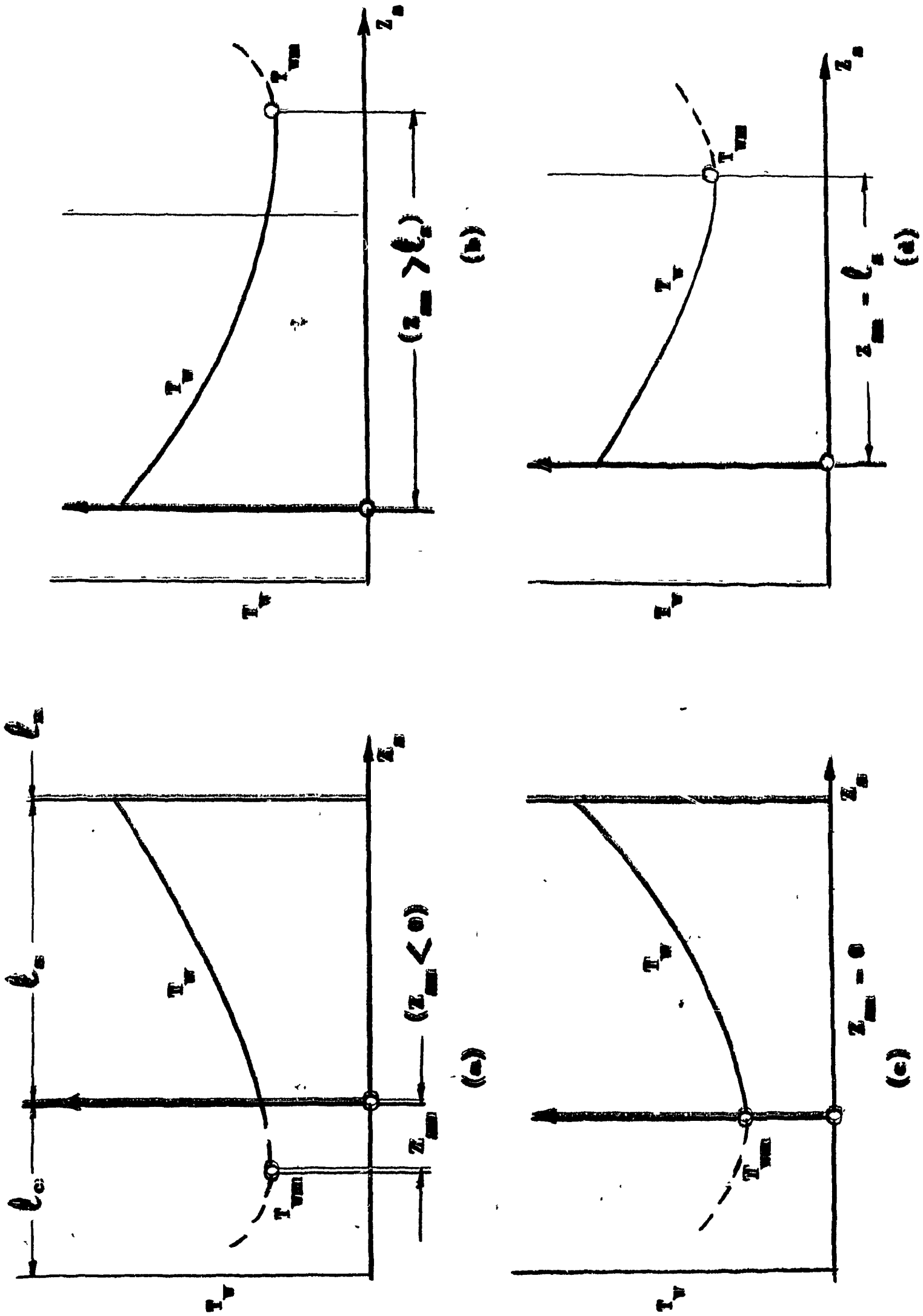
Fig. (10): Temperature Distribution in the Subcooled Region under Different Conditions.
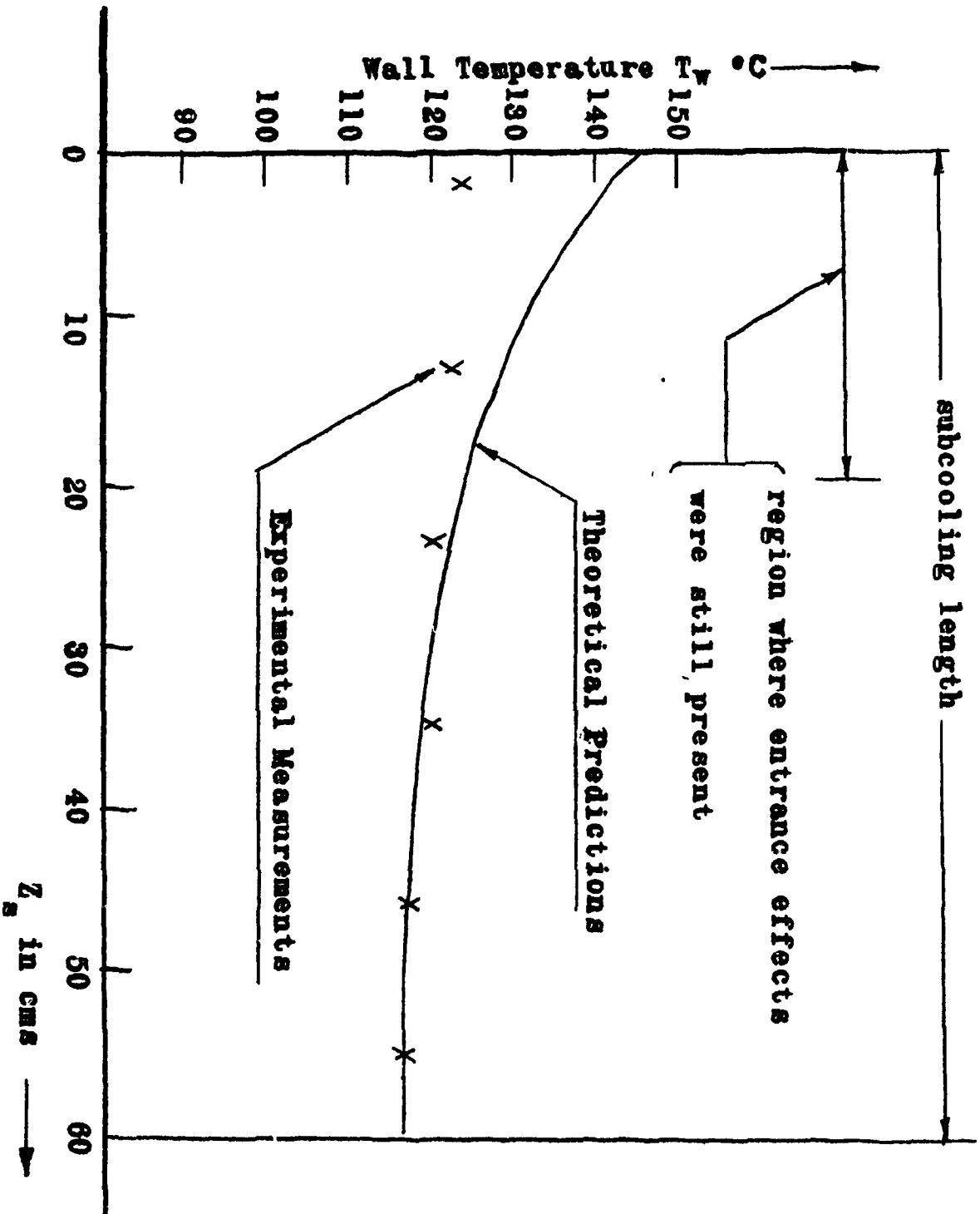
Fig. (11): Surface Temperature in The Subcooled Region.
Experimental Run 10.58 watt/cm^2, 91°C Inlet Temperature.
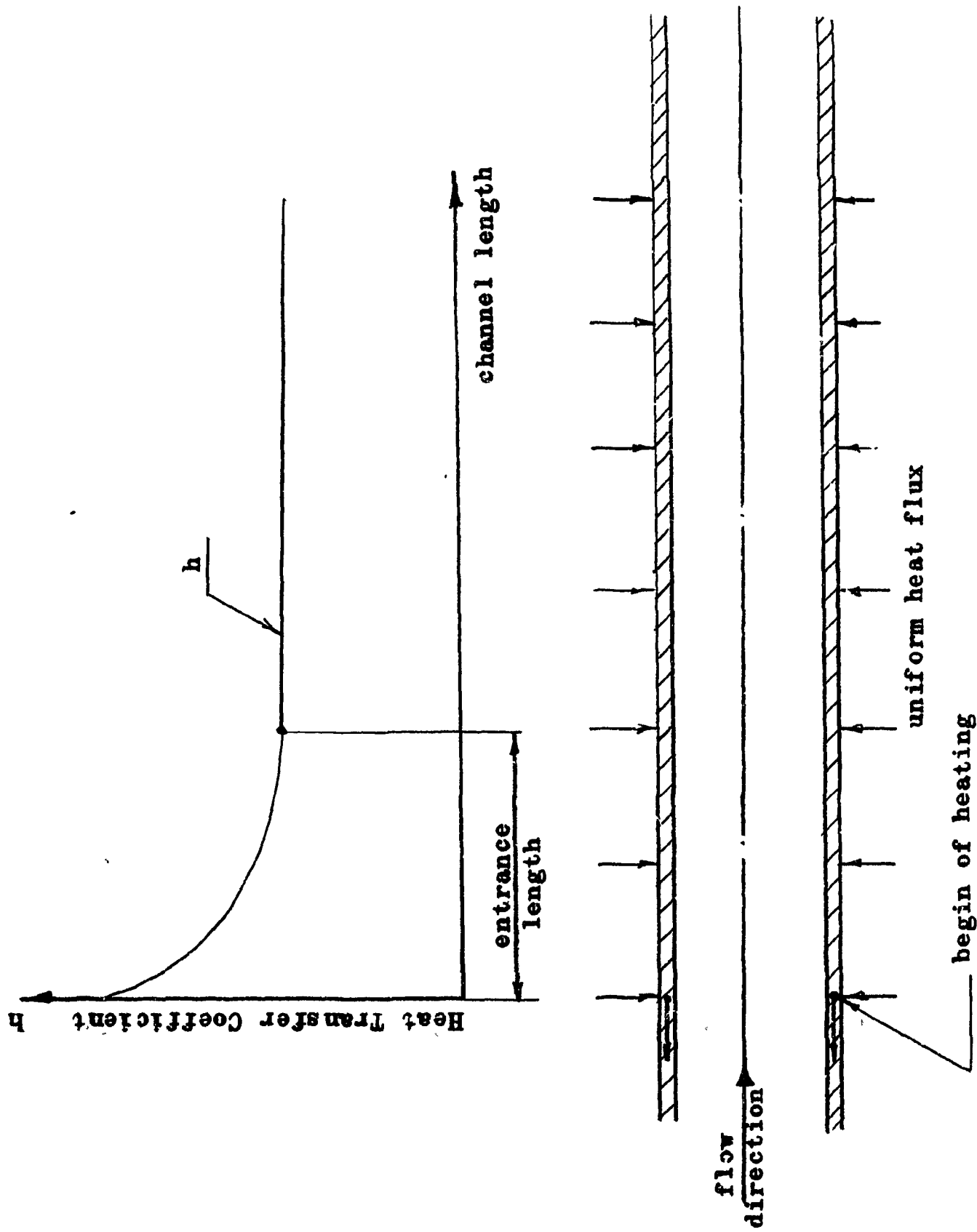
Fig. (12): Heat Transfer Coefficient Distribution in a Uniformly Heated Channel.
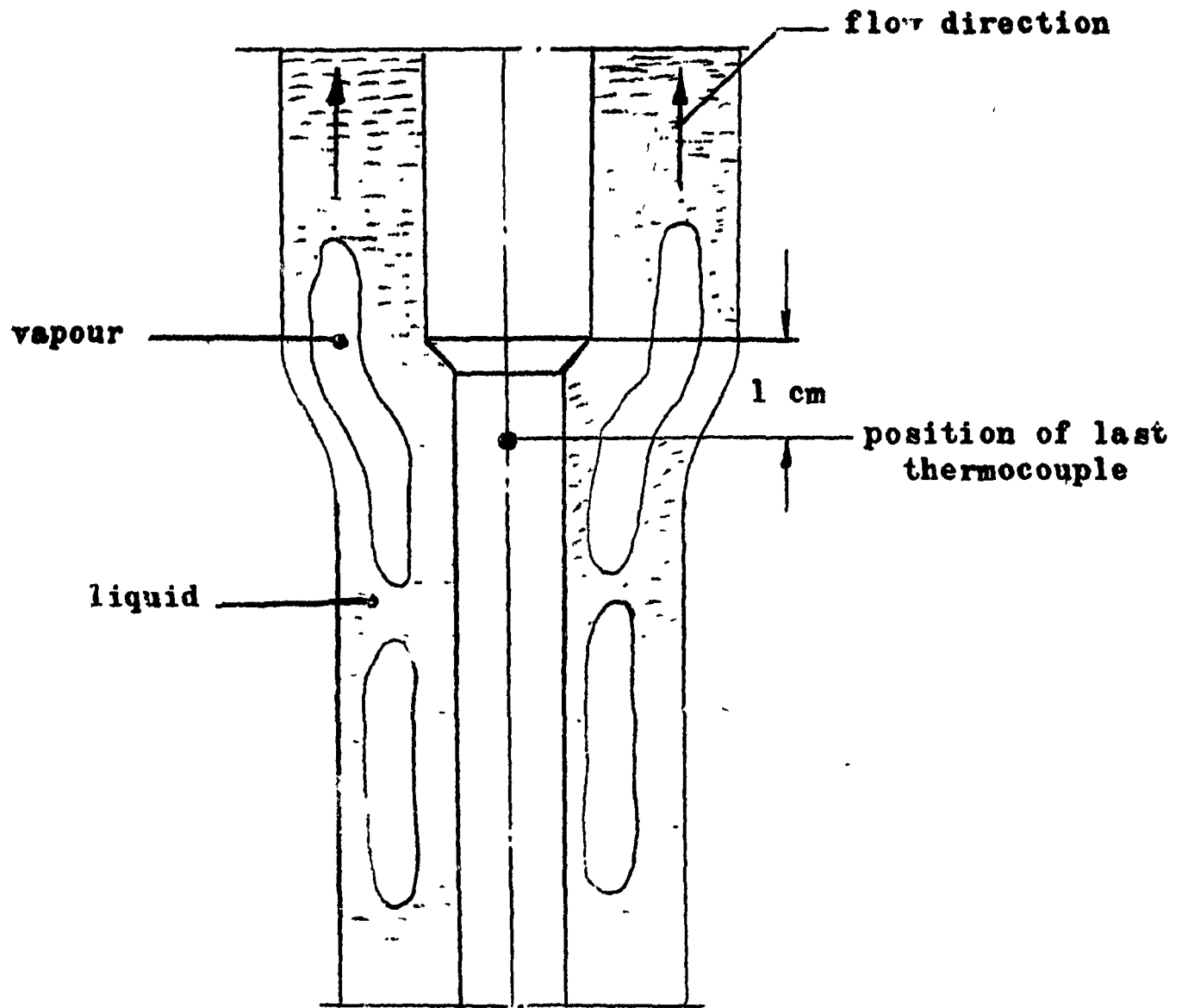
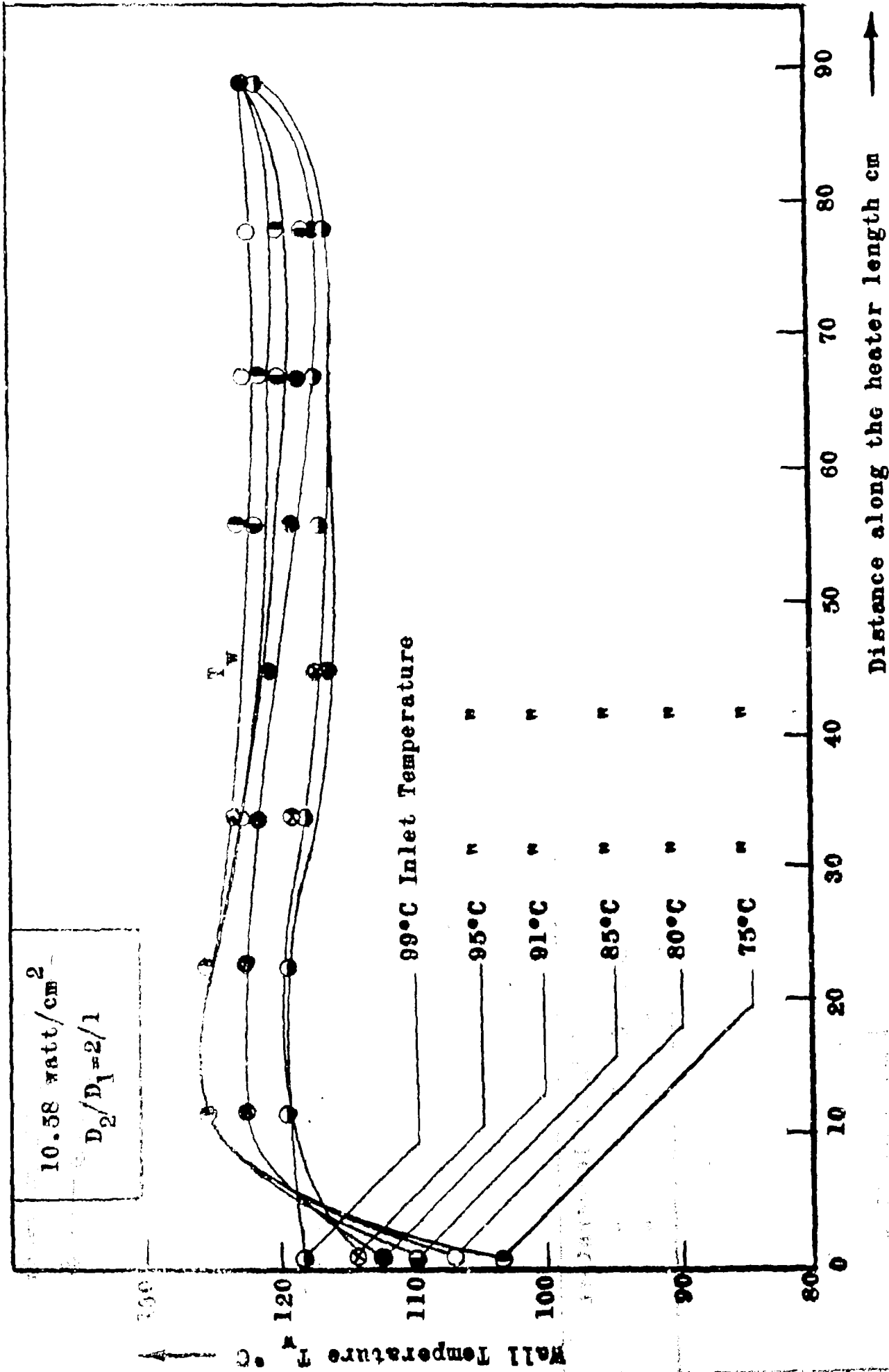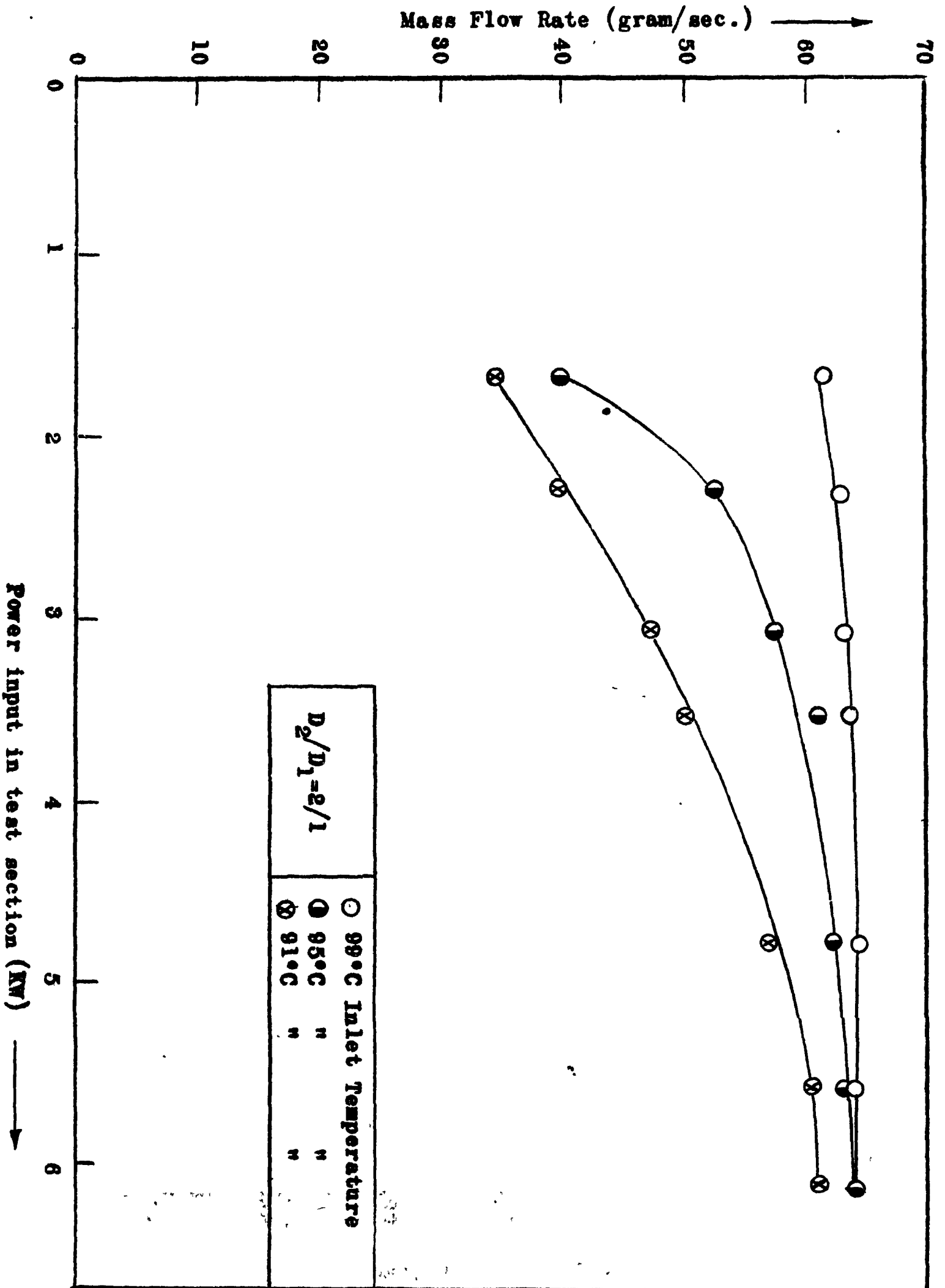Fig. (13): Flow Pattern at The Outlet in The Two Phase Runs.

Fig. (14): Experimental Runs at 10.58 watt/cm².

Fig. (15): Mass Flow Rate Versus Power Input.
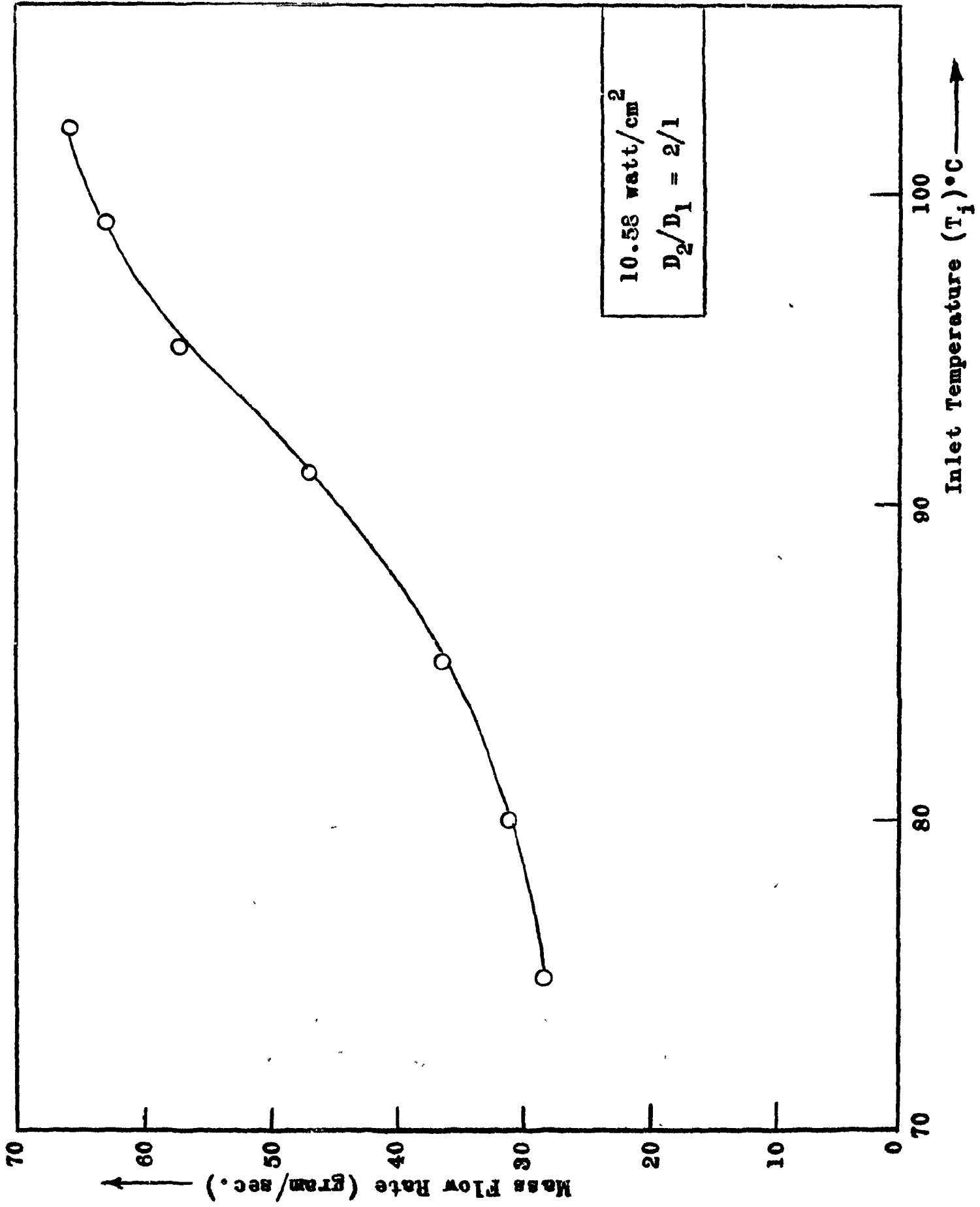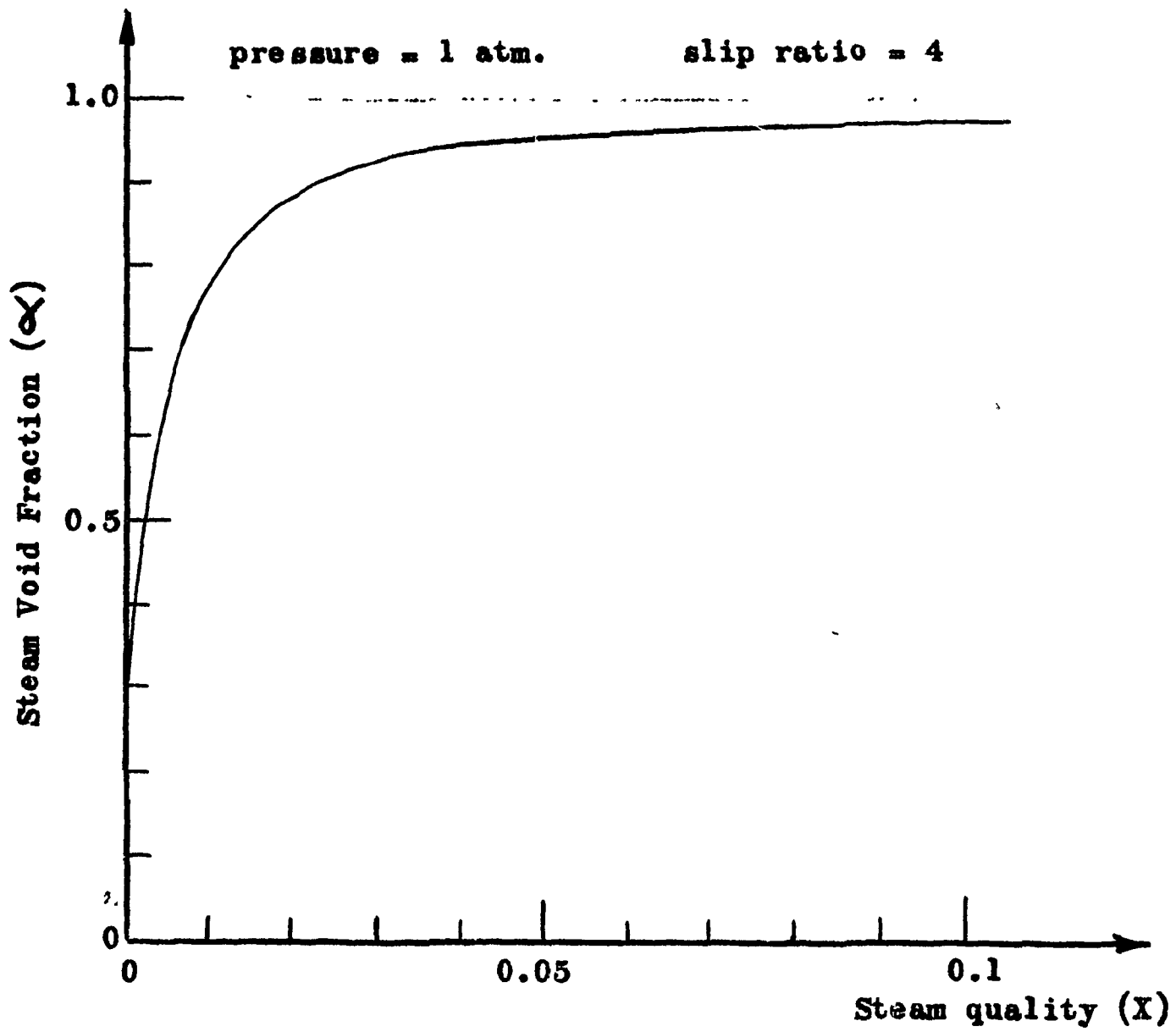
Fig. (16): Mass Flow Rate Versus Inlet Temperature.

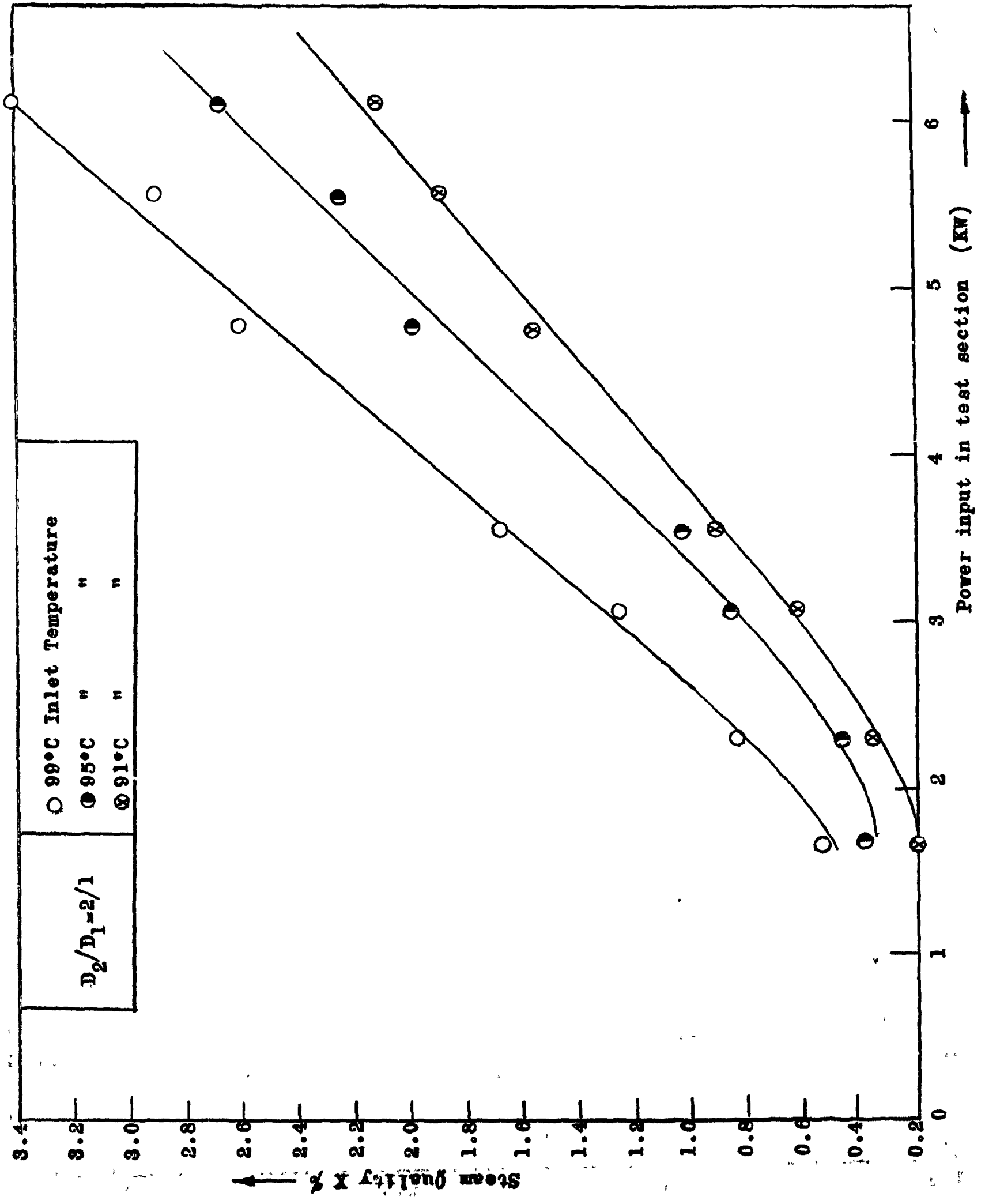Fig. (17): Relation between Steam Void Fraction and Steam Quality for a Two Phase flow at Atmospheric Conditions.
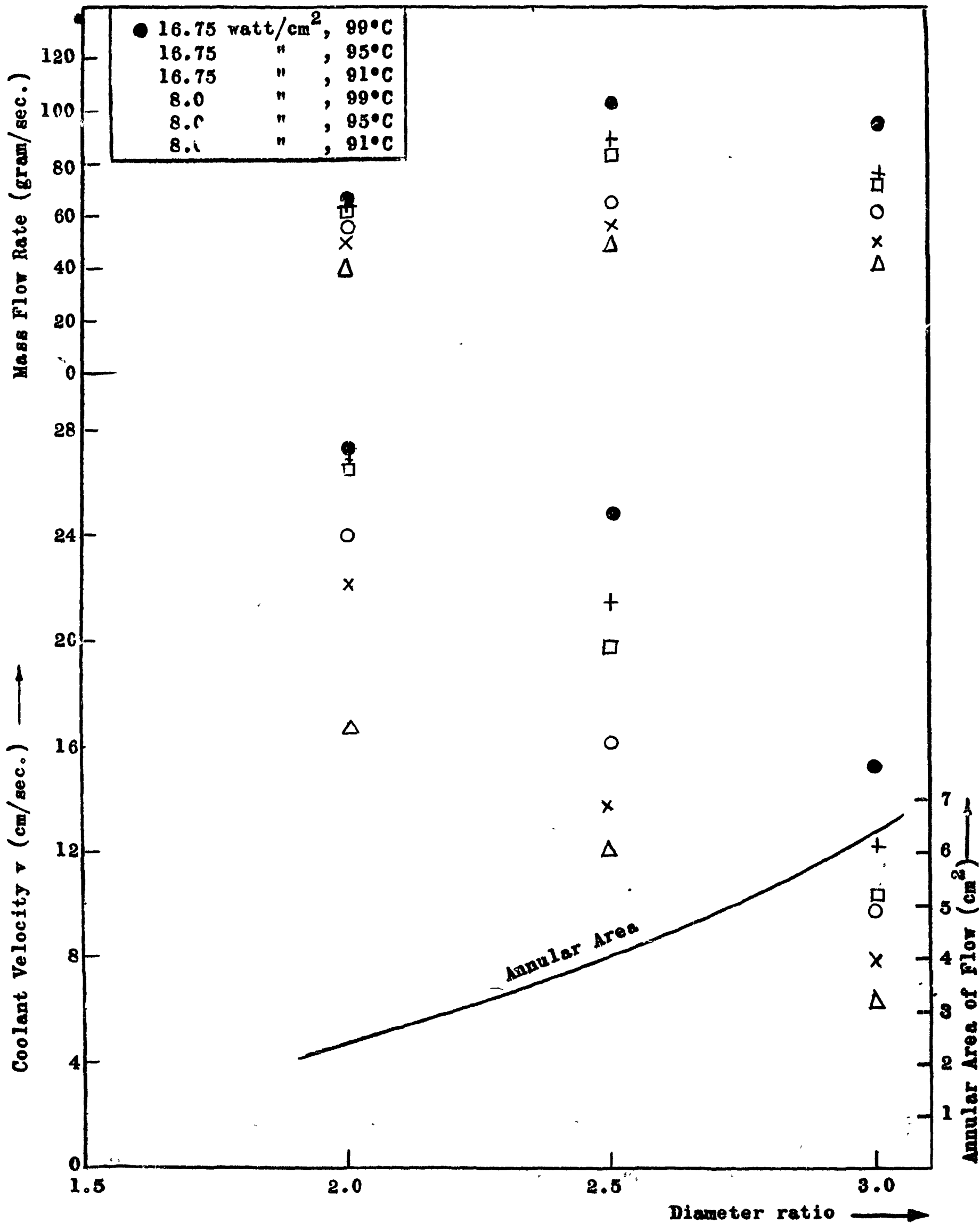
Fig. (18): Steam Quality Versus Power Input.

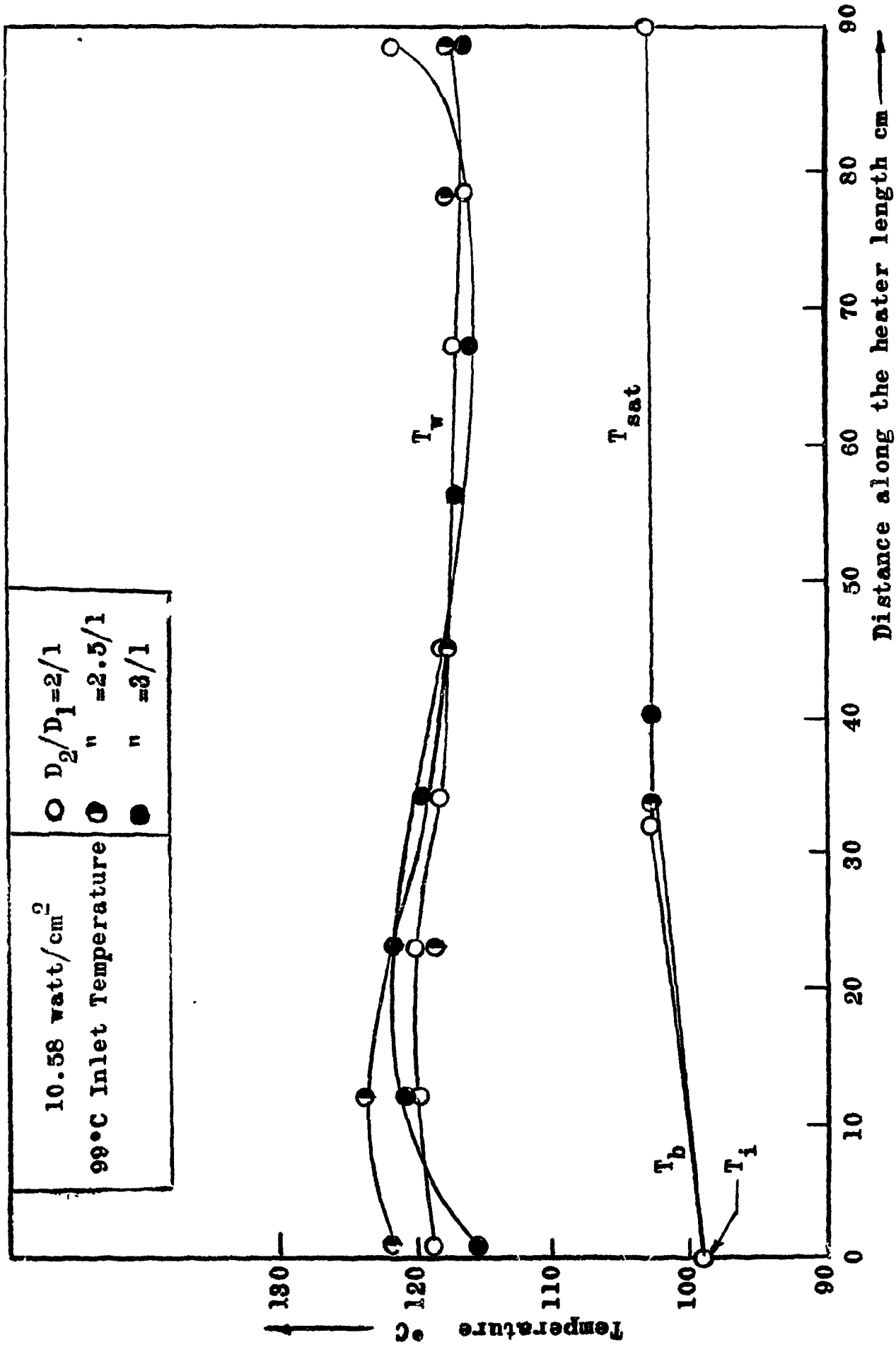Fig. (19): Effect of Diameter Ratio on The Coolant Mass Flow Rate.

Fig. (20): Wall Surface Temperature Distribution at Different Diameter Ratios.

R E F E R E N C E S

/¯1/ M.F. El-Fouly and M.S. Khattab: "An Experimental Loop for Two Phase Heat Transfer Investigations", U.A.R.A.E.E./Rep.-81, 1969.

/¯2/ M.S. Khattab: "Heat Transfer Between Reactor Fuel Rods and Two Phase Coolant", M.Sc. Thesis, to be submitted to the Faculty of Engineering, Cairo University, by the end of 1970.

/¯3/ E.J. Davis and G.H. Anderson: "The Incipience of Nucleate Boiling in Forced Convection Flow", A.I.ch.E. Journal, July, 1966.

/¯4/ A.M. Mitry: "Heat Transfer in Annular Reactor Channels Steady State Forced Convection in the Transition and Turbulent Regions", M.Sc. Thesis, Submitted to the Faculty of Engineering, Cairo University, 1968.

/¯5/ L. Sani: "Analysis of Design Criteria for Boiling Water Reactors", Atomic Energy Review, Volume 1, Number 3, Vienna 1963.

APPENDIX

The relation between the steam quality (X) and the steam volume fraction (α) may be obtained from the continuity equation, or

$$\left(\frac{X}{1-X}\right) = \frac{\rho_v}{\rho_\ell} \ S \ \left(\frac{\alpha}{1-\alpha}\right) \tag{A-1}$$

This equation can be rearranged as

$$\alpha = \frac{1}{1 + S\left(\frac{\rho_v}{\rho_\ell}\right)\left(\frac{1-X}{X}\right)} \tag{A-2}$$

The slip ratio (S) varies according to the system pressure, steam quality and superficial velocity. Taking an average value of 4 $\boxed{5}$, and substituting for ρ_v and ρ_ℓ at atmospheric conditions give

$$\alpha = \frac{1}{1 + 2.4 \times 10^{-3}\left(\frac{1-X}{X}\right)} \tag{A-3}$$

and is plotted in Fig. (17) in the report.